

AKADEMIA GÓRNICZO-HUTNICZA
IM. STANISŁAWA STASZICA W KRAKOWIE

AGH UNIVERSITY OF SCIENCE
AND TECHNOLOGY

AGH

HIGH TEMPERATURE CORROSION IN MULTICOMPONENT AGGRESIVE ENVIRONMENTS

<http://home.agh.edu.pl/~grzesik>



AGH

Literature

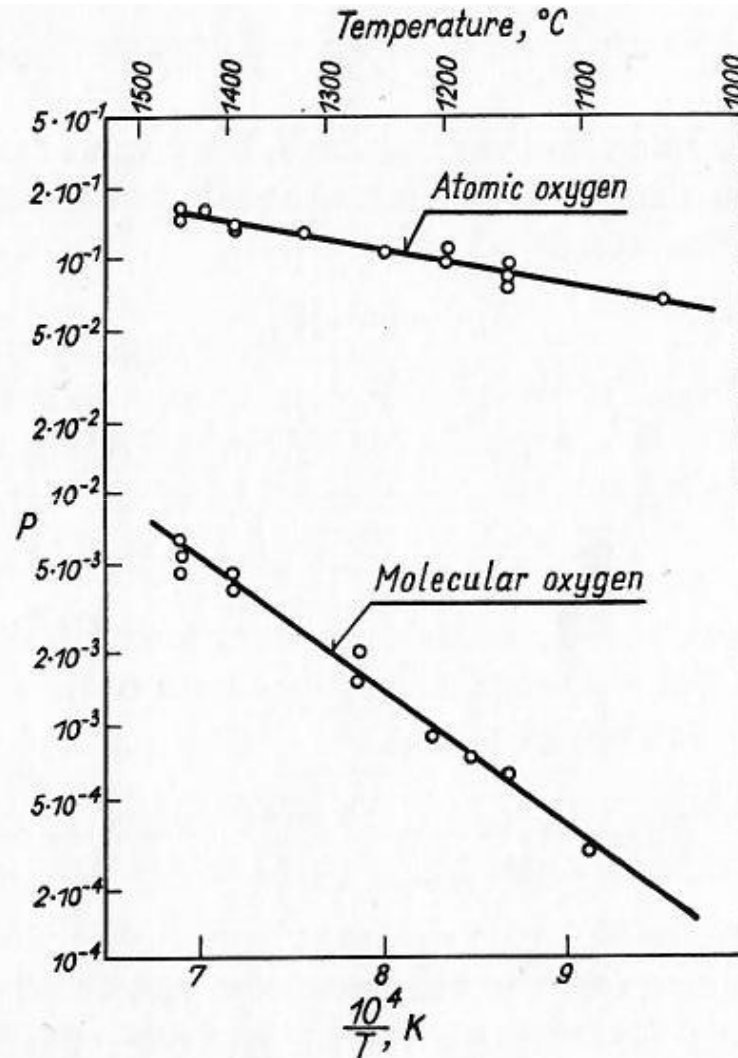
1. P. Kofstad, „High-Temperature Corrosion”, John Wiley & Sons, Inc, New York-London-Sydney, 1988.
2. S. Mrowec, Kinetyka i mechanizm utleniania metali, 1980.
3. S. Mrowec, „An Introduction to the Theory of Metal Oxidation”, National Bureau of Standards and the National Science Foundation, Washington, D.C., 1982.
4. S. Mrowec and T. Werber, Modern Scaling-Resistant Materials, National Bureau of Standards and National Science Foundation, Washington D.C., 1982.
5. A.S. Khanna, „Introduction to High Temperature Oxidation and Corrosion”, ASM International, Materials Park, 2002.
6. Wei Gao and Zhengwei Li ”Developments in high-temperature corrosion and protection of metals”, Ed, Woodhead Publishing Limited, Cambridge, England, 2008.
7. N. Birks, G.H. Meier and F.S Pettit, Introduction to the high temperature oxidation of metals, Cambridge, University Press, 2009.
8. D. J. Young, „High temperature oxidation and corrosion of metals”, Elsevier, Sydney 2016.

Oxidation in different oxidizing atmospheres

The same aggressive element can be present in the form of different molecules or form aggressive chemical compounds. The most common aggressive element (oxygen) is usually found as molecular oxygen O_2 , but can also be present as atomic oxygen, O , or form compounds with other elements, e.g. H_2O , CO , CO_2 , SO_2 , etc.

Depending on its form, an aggressive component can influence the rate and mechanism of high temperature corrosion.

Mo oxidation in two oxidizing atmospheres

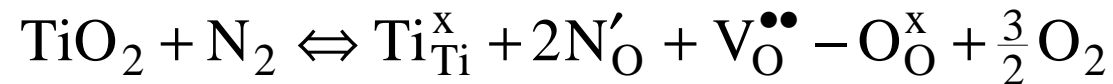


P – parameter being the measure of oxidation rate at the same oxidant pressure

Oxidation in air atmosphere (21% O₂ and 79% N₂)

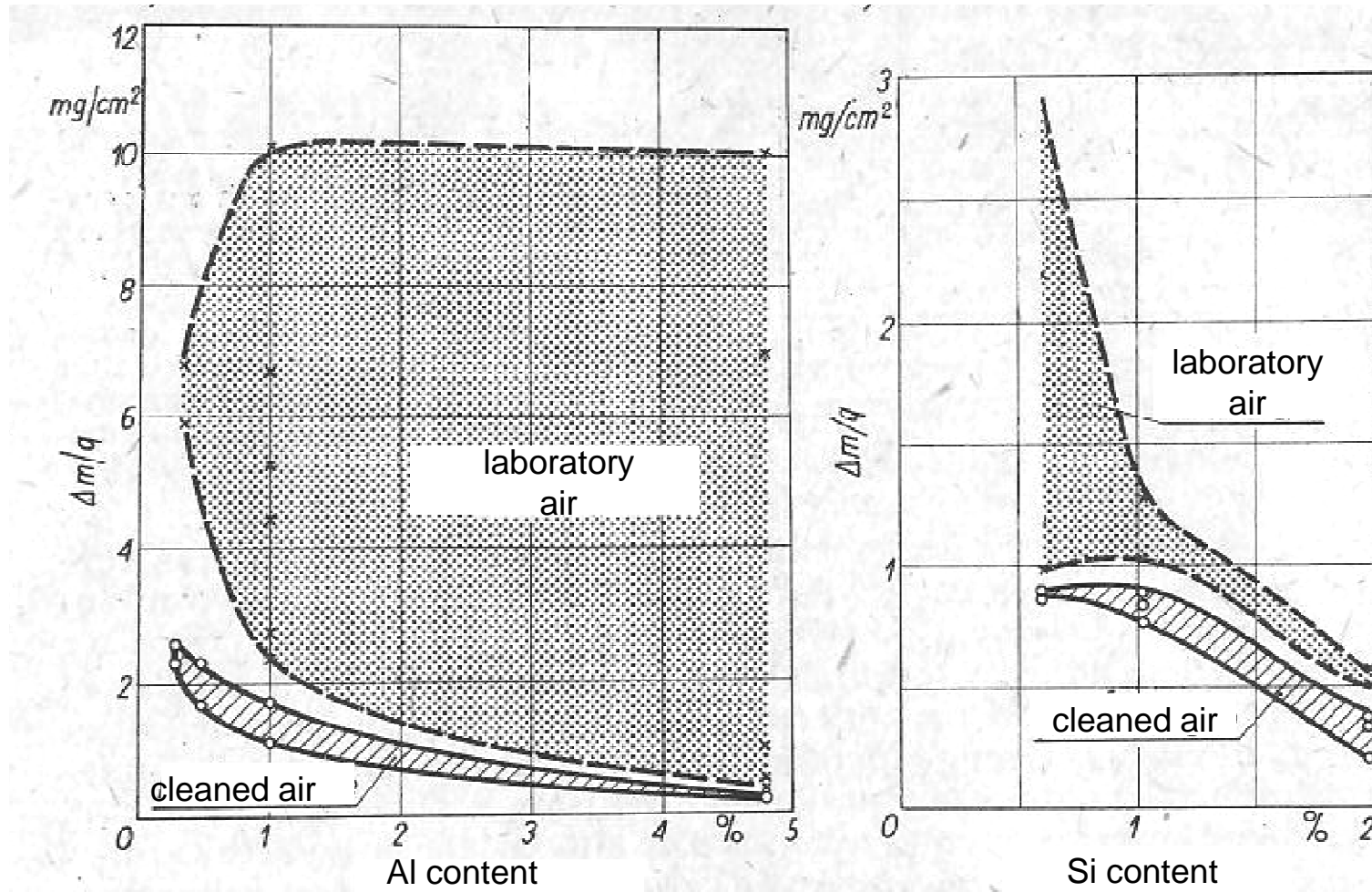
The role of nitrogen in high temperature metal corrosion processes in air:

- enables nitride formation
- influences intrinsic defect concentration by doping the anion sublattice of the oxide, e.g. increases anion vacancy concentration in TiO₂:

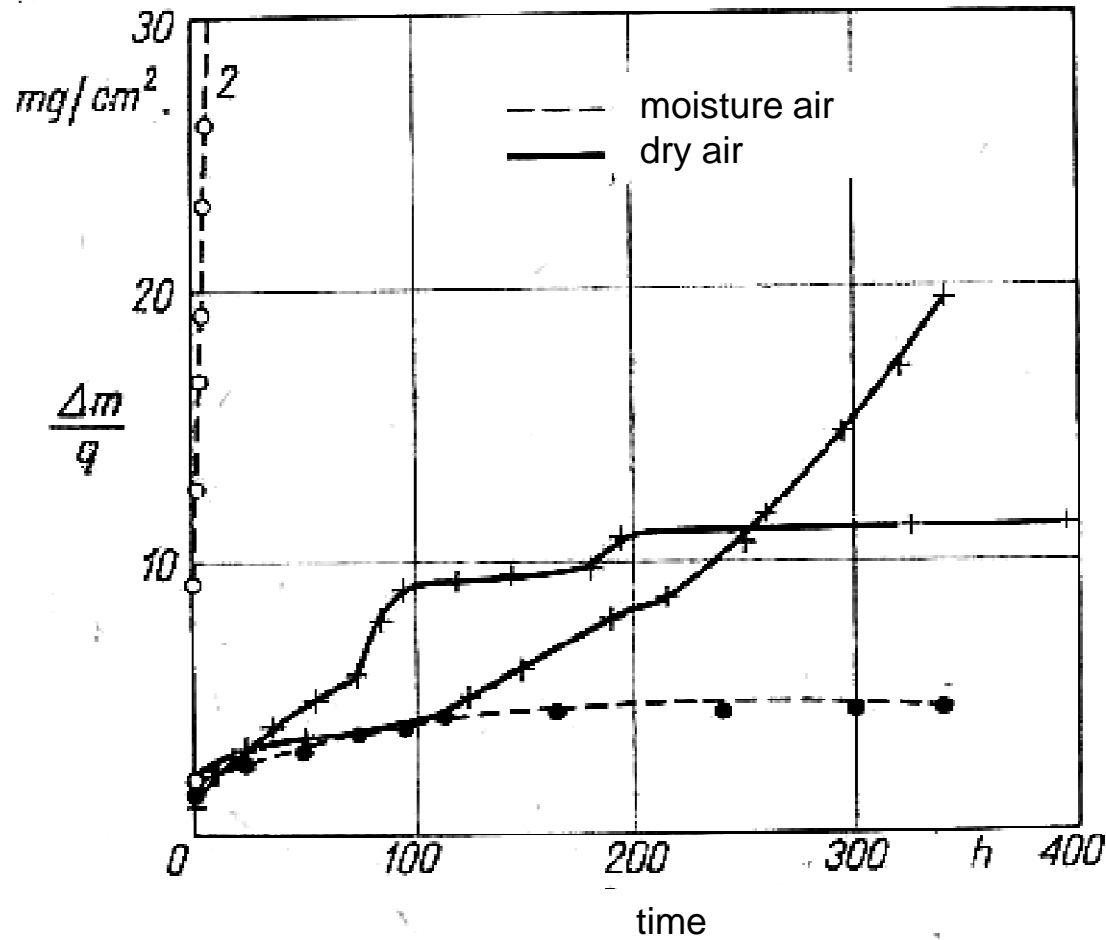


- influences corrosion process kinetics

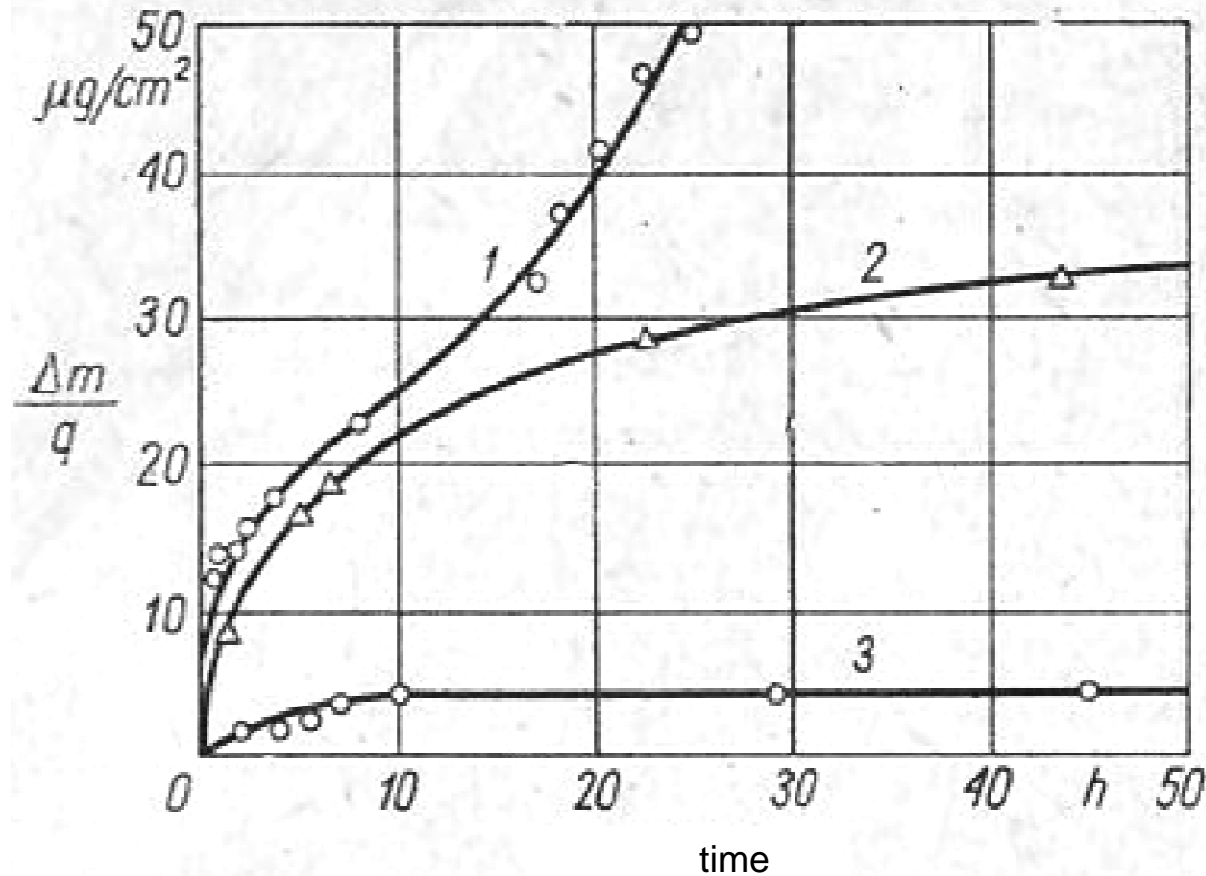
Mass gains of oxidized Fe-Al and Fe-Si alloys in laboratory and specially cleaned air (700 °C, 24 h)



Influence of moisture in air on oxidation kinetics of chromium-nickel steels at different temperatures



Influence of organic impurities in air on Mg oxidation kinetics at 525 °C

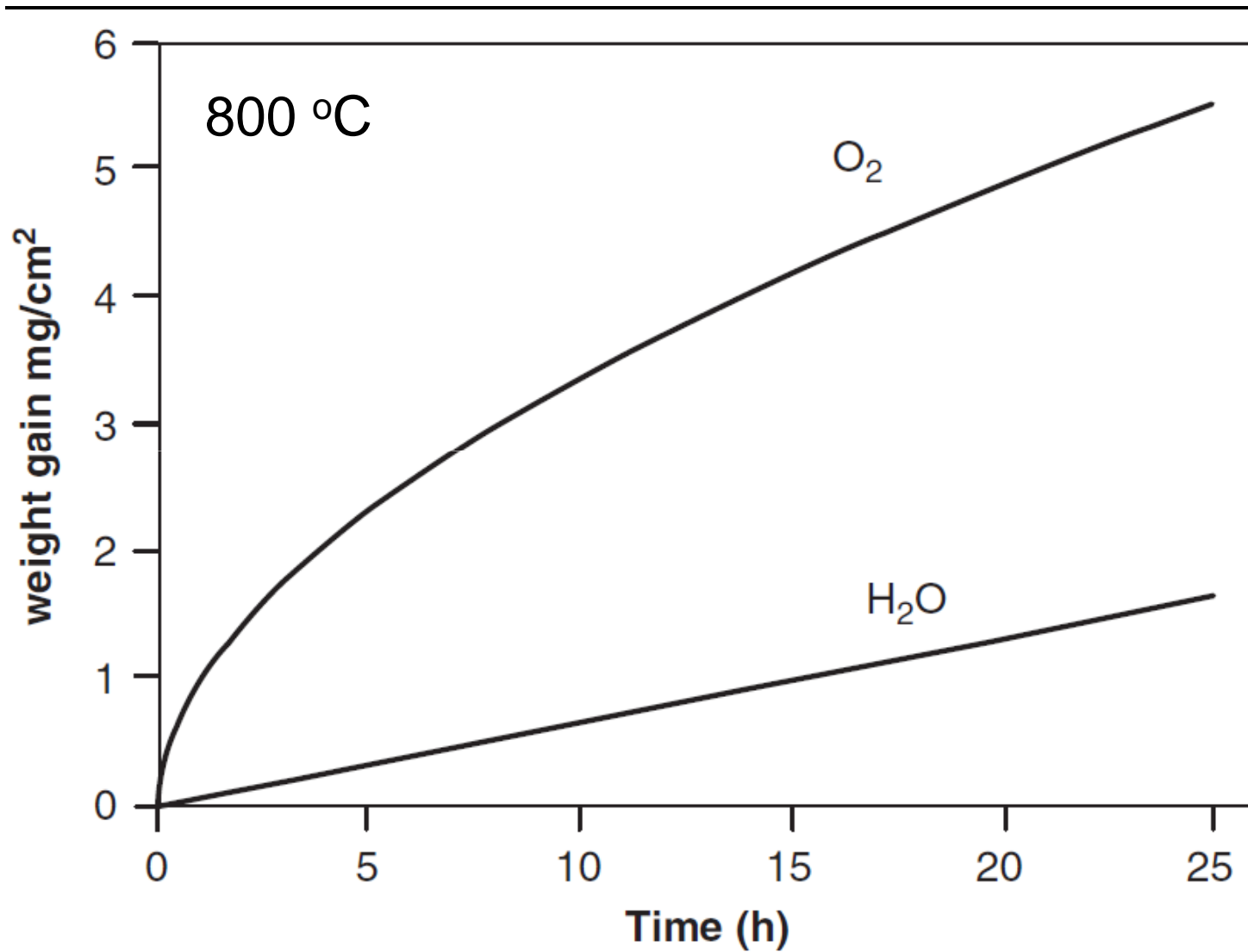


- 1 – oxygen + 0,5% n-nonane
- 2 – unclean oxygen from grease vapors
- 3 – specially cleaned oxygen

Role of water vapor in oxidation

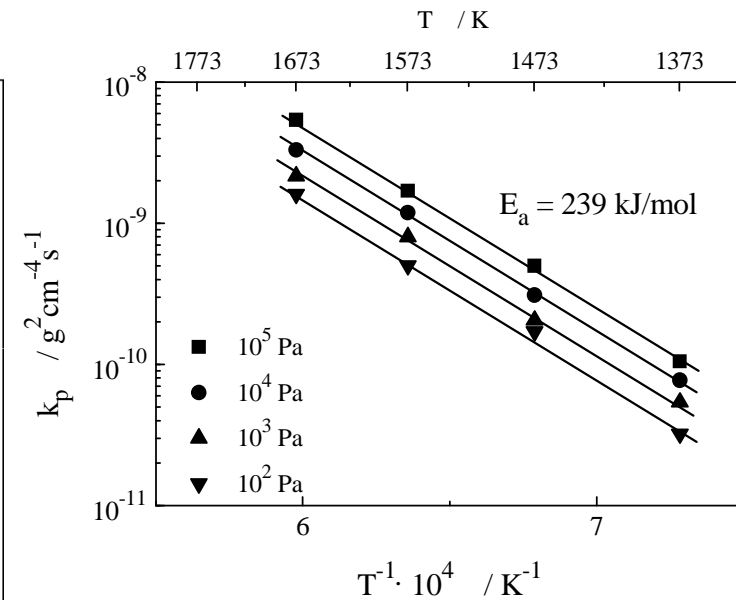
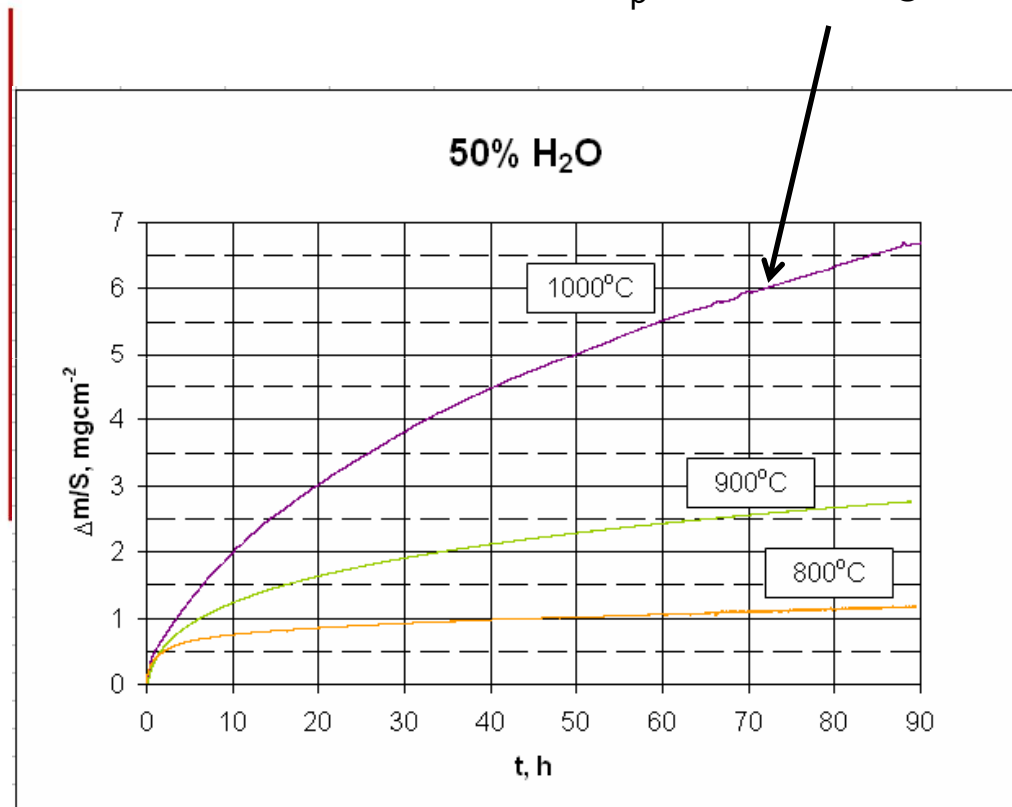
- decarburization of alloys due to hydrogen
- worsening of material physical properties
- at high water vapor temperatures and pressures the corrosion mechanism is similar to the electrochemical corrosion mechanism
- as a rule, selective oxidation of alloys
- change in corrosion mechanism and rate
- enabling the formation of volatile metal hydroxides
- most steels oxidize in water vapor or air, or exhaust gases containing water vapor faster than in “dry” air.

Nickel oxidation kinetics in oxygen and water vapor



Nickel oxidation kinetics in O₂-50%H₂O atmosphere

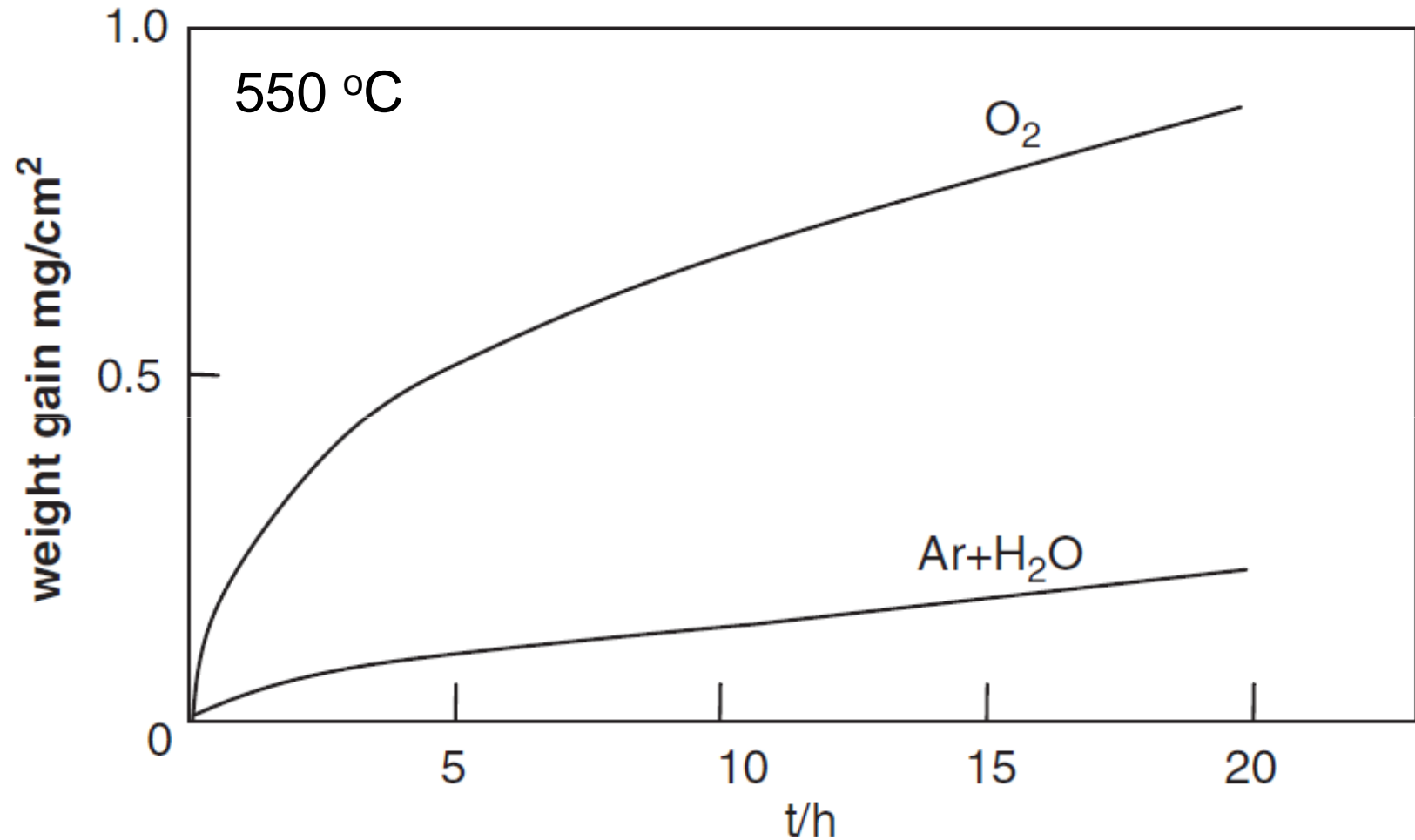
$$k_p = 1,4 \cdot 10^{-10} \text{ g}^2 \text{ cm}^{-4} \text{ s}^{-1}$$



S. Mrowec, Z. Grzesik,
Journal of Physics and Chemistry
of Solids, 65, 1651-1657 (2004).

Klaudia Wrona, Master Thesis „Utlenianie niklu w atmosferach zawierających parę wodną”, AGH, Kraków, 2009

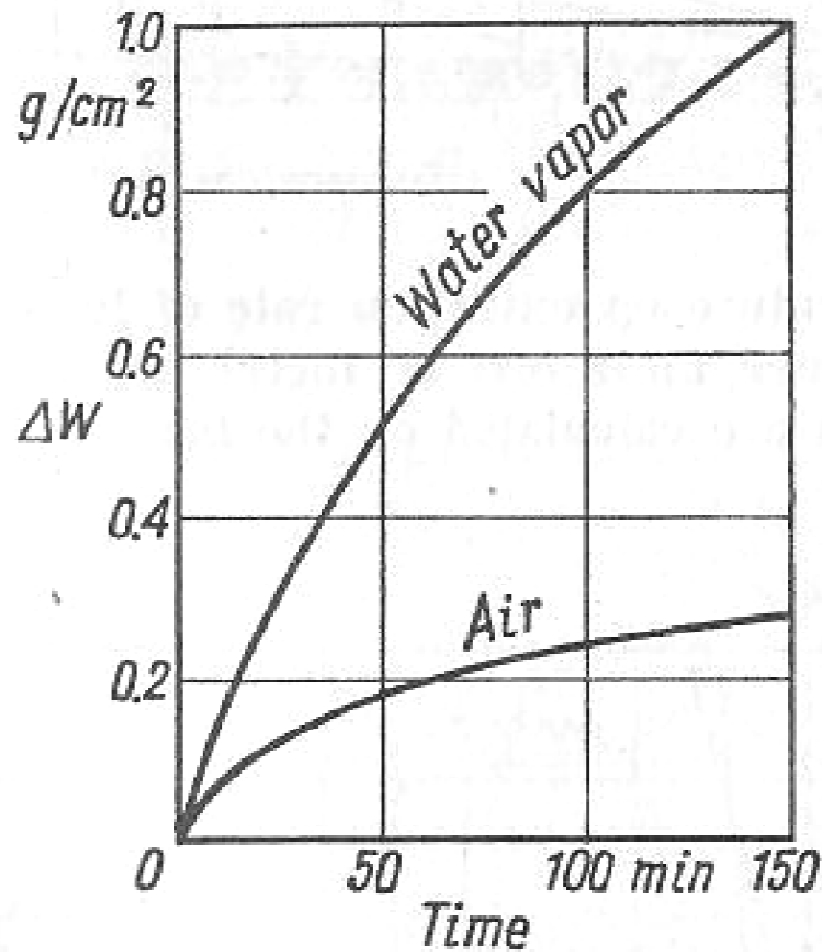
Oxidation kinetics of iron in oxygen and an argon-water vapor mixture



Influence of water vapor on the oxidation rate of carbon steels

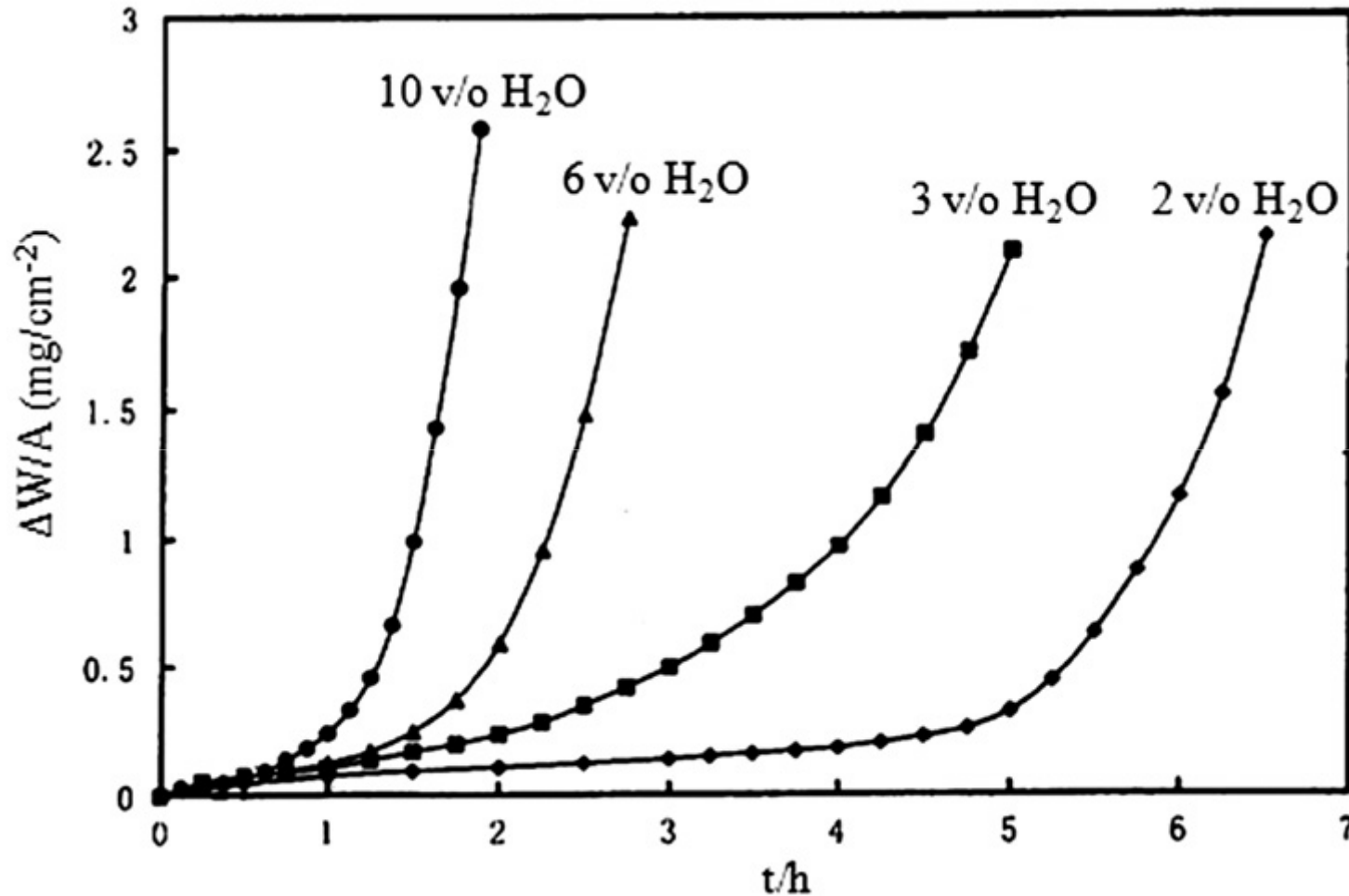


www.agh.edu.pl

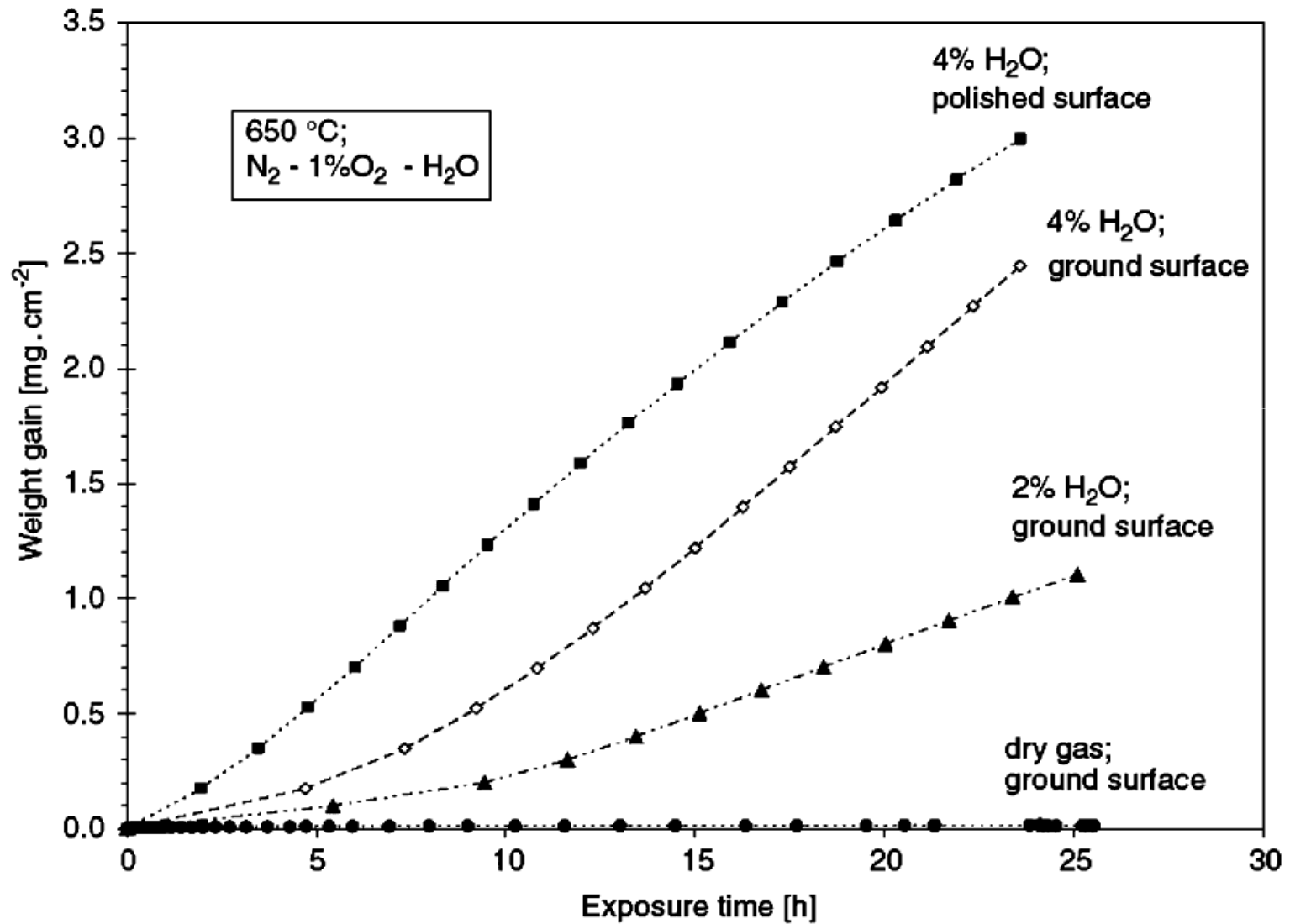


S. Mrowec and T. Werber, Modern Scaling-Resistant Materials, National Bureau of Standards and National Science Foundation, Washington D.C., 1982

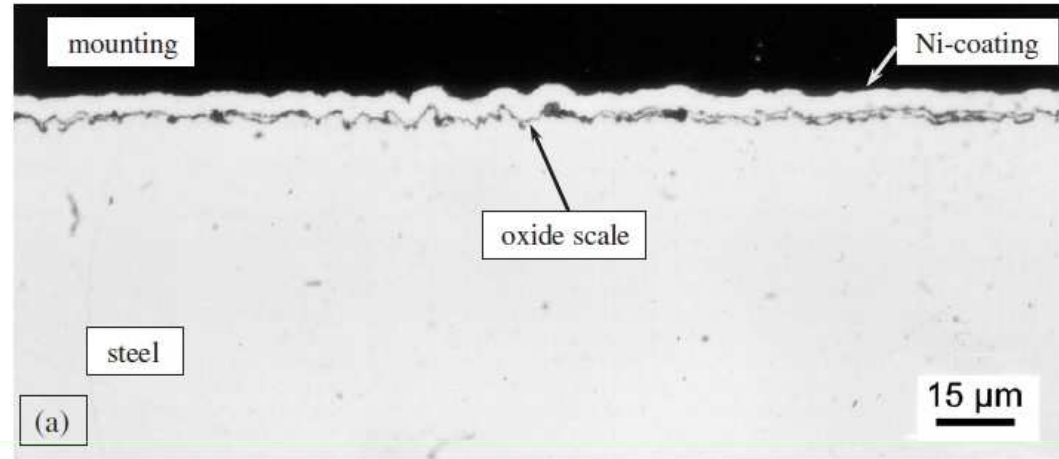
Influence of water vapor on the oxidation rate of Fe-15Cr steel in oxygen at 900 °C



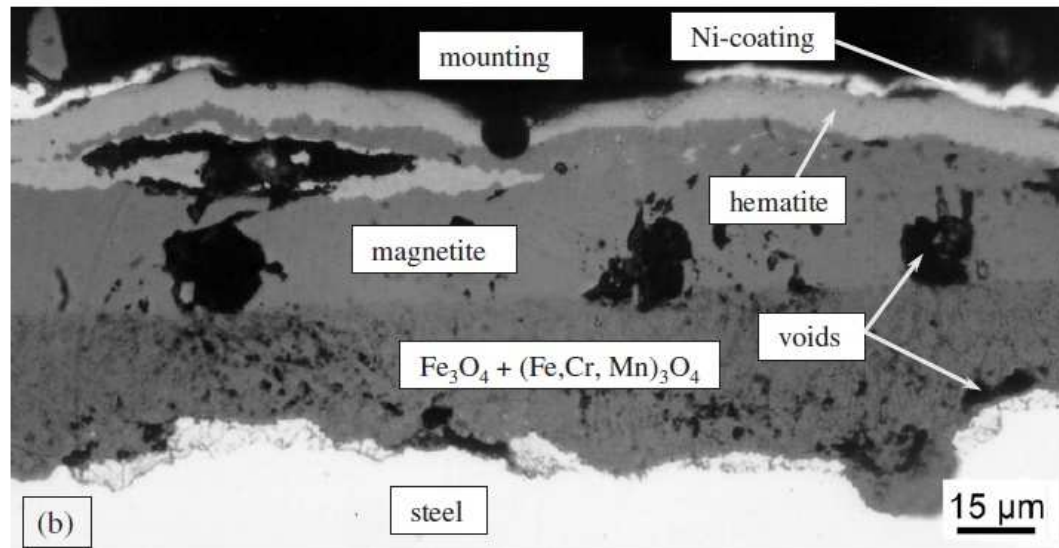
Influence of water vapor on the oxidation rate of boiler steel P91



Influence of water vapor on the morphology of the scale formed on a P91 boiler steel sample oxidized for 100 h at 650 °C

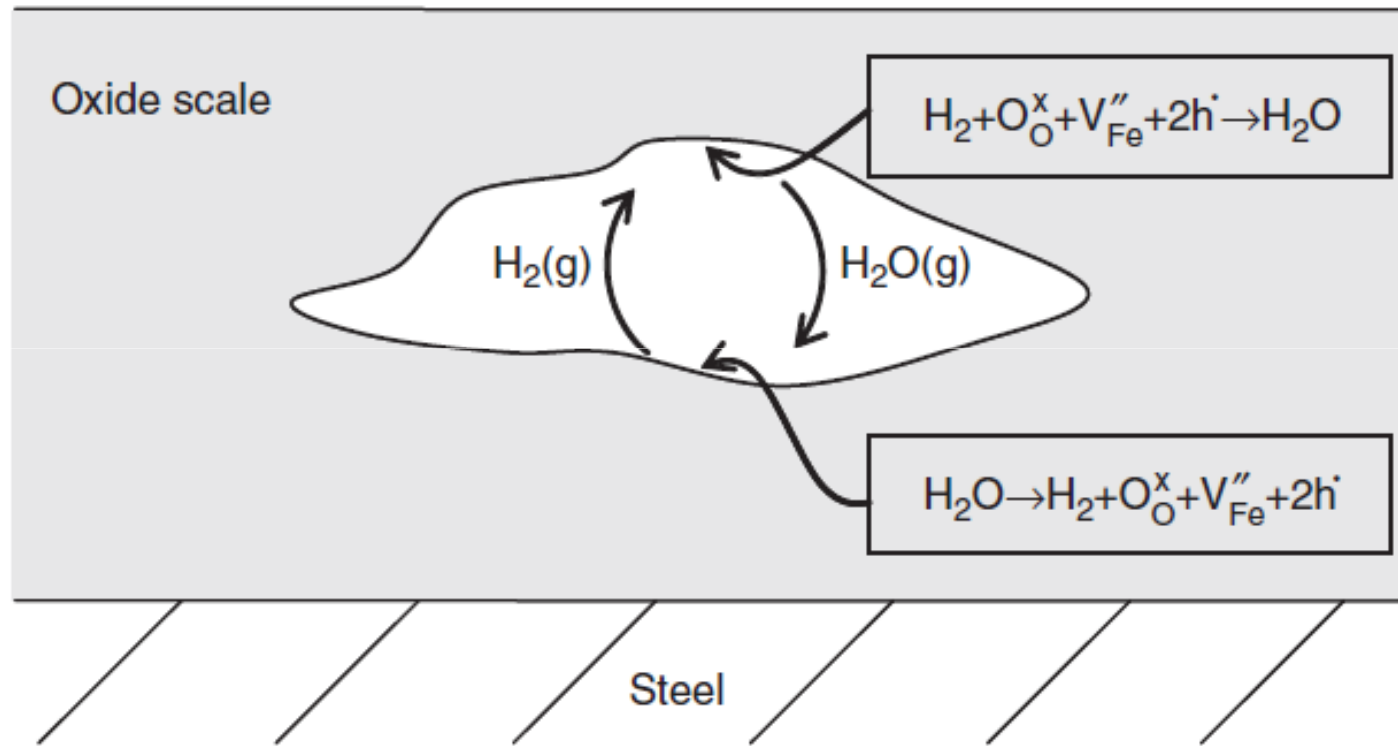


$N_2-1\%O_2$

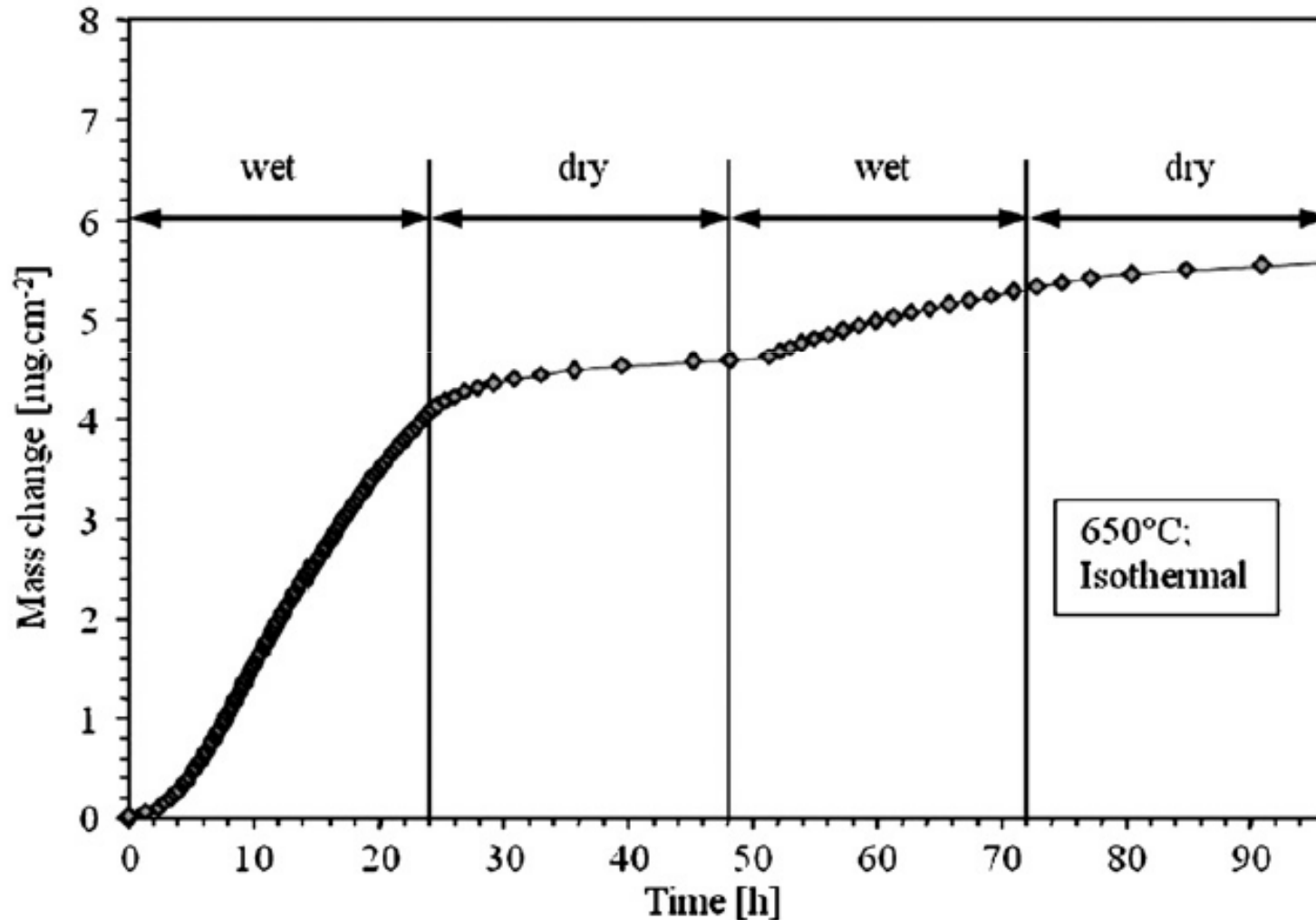


$N_2-1\%O_2-2\% H_2O$

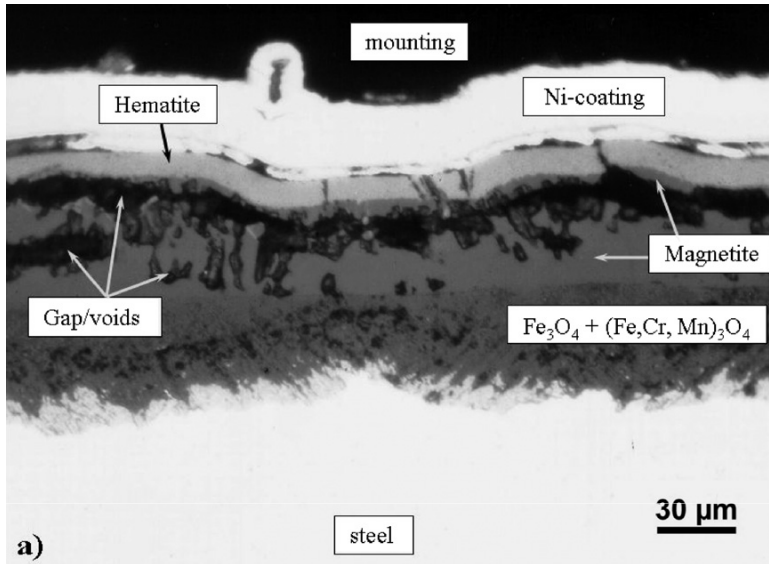
Schematic illustration of oxygen transport through water vapor in a porous scale formed on diluted Fe-Cr alloys



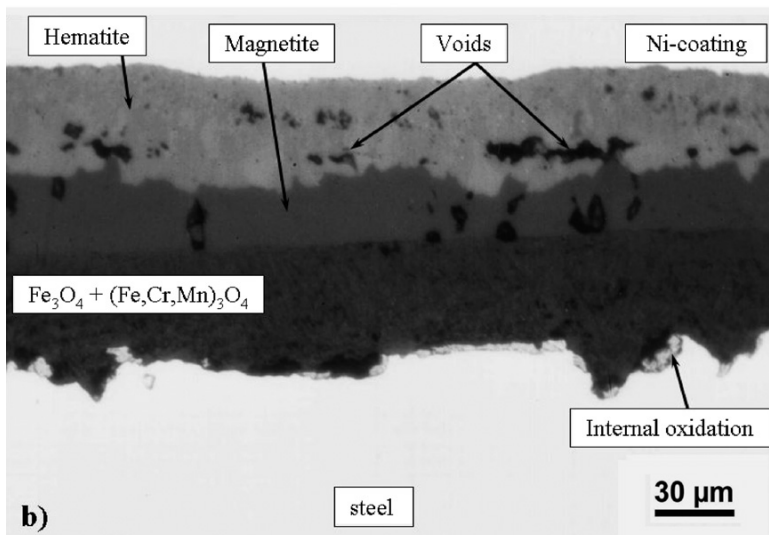
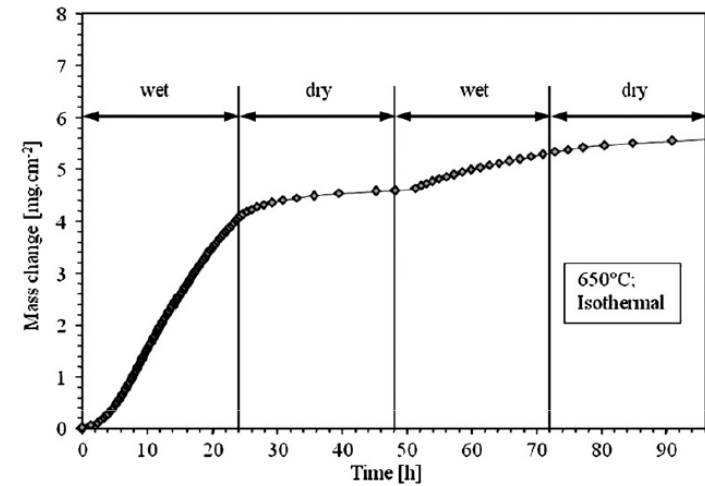
Oxidation kinetics of P91 steel at 650 °C in an atmosphere with an alternating composition of N₂-1%O₂-4%H₂O (wet) and N₂-1%O₂ (dry)



Cross-sections of scales formed on P91 steel at 650 °C in N₂-1%O₂-4%H₂O (a) and N₂-1%O₂ (b)



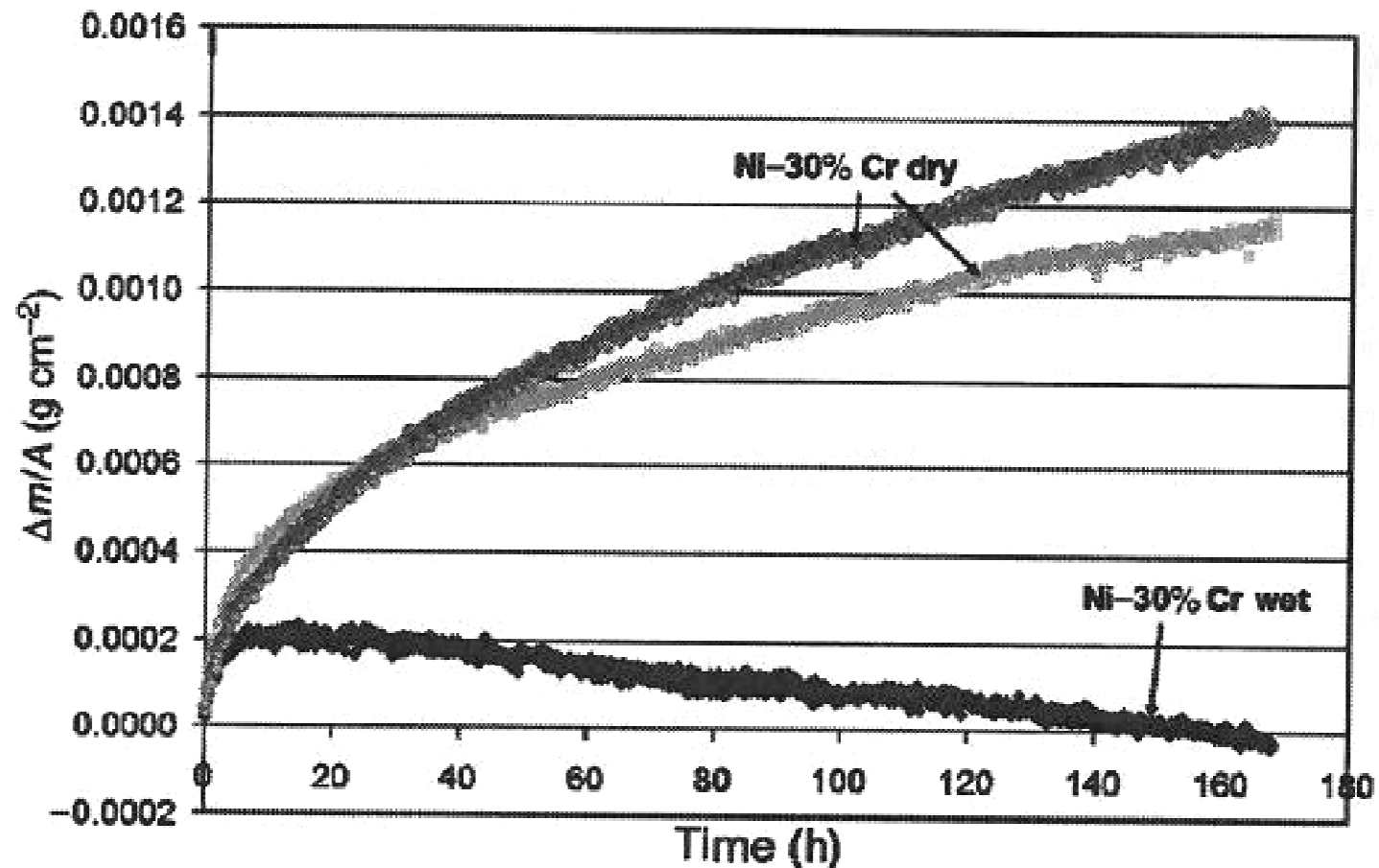
t = 24 h



t = 48 h

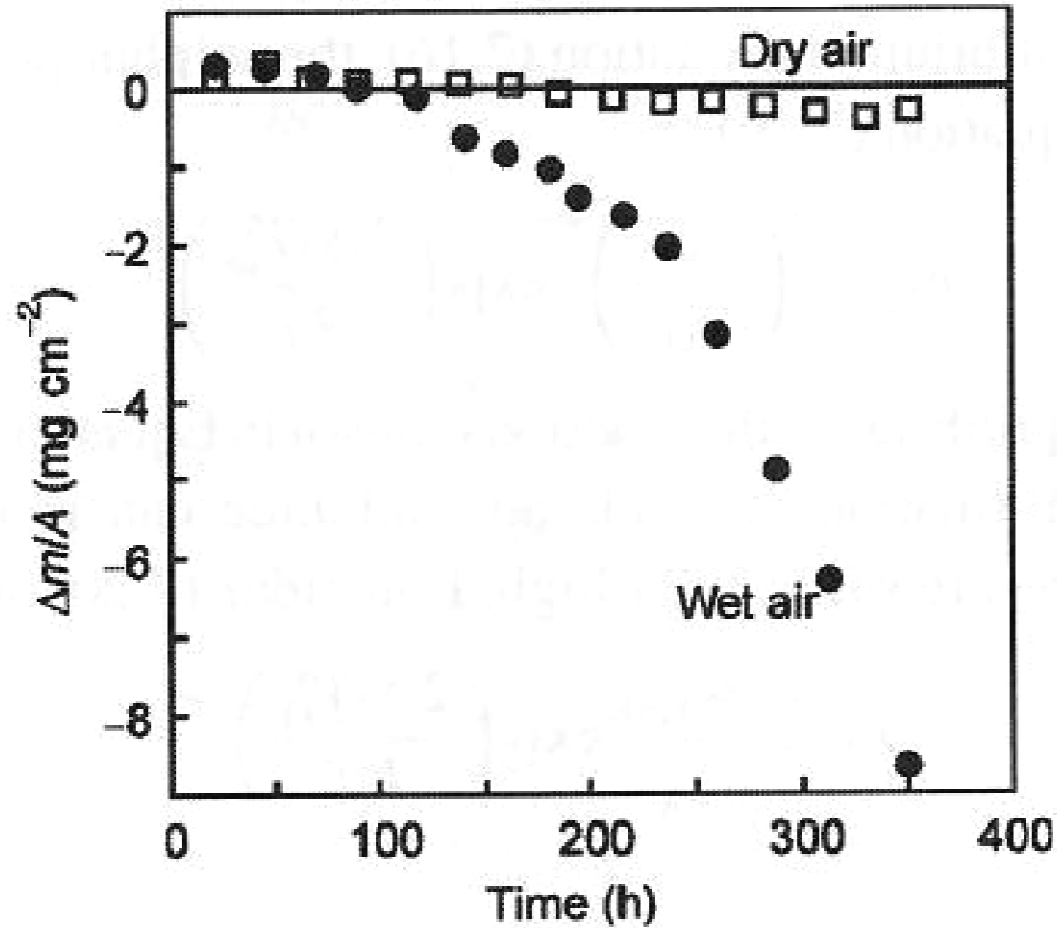
- ⇒ decrease in porosity
- ⇒ conversion of Fe₃O₄ to Fe₂O₃
- ⇒ improvement in scale protective properties

Influence of water vapor on the oxidation rate of Ni-30 %wt. Cr steel at 900 °C

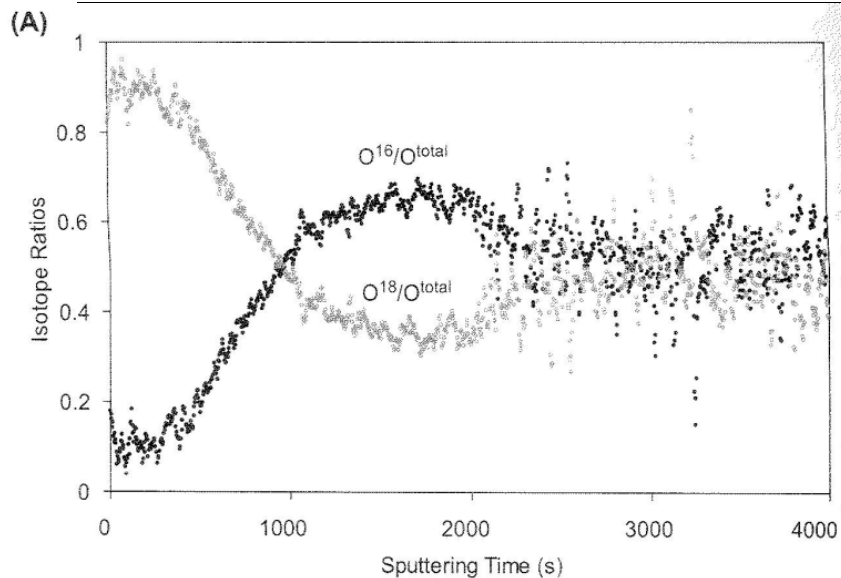


N. Birks, G.H. Meier and F.S Pettit, Introduction to the high temperature oxidation of metals, Cambridge, University Press, 2009.

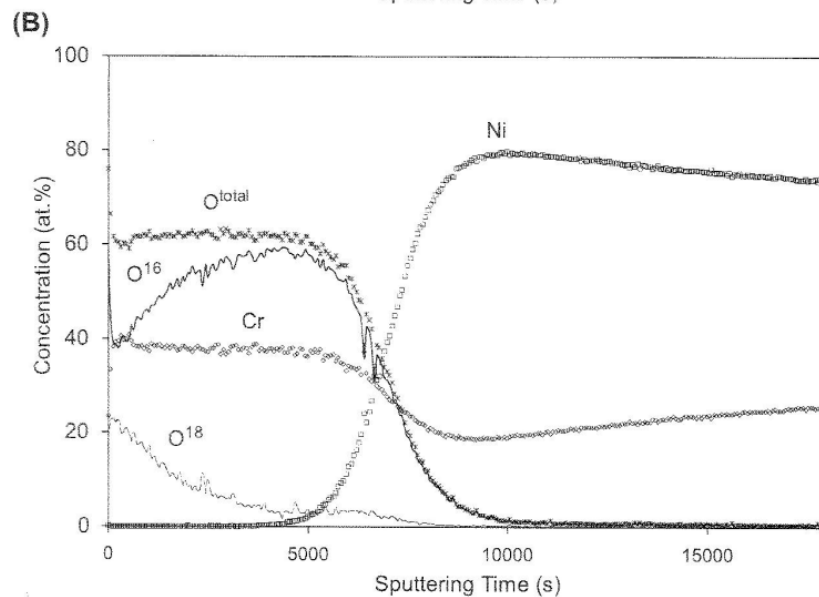
Influence of water vapor on the oxidation rate of CMSX-4 alloy in cyclic conditions (25 - 1100 °C)



Concentration profiles of O^{16} and O^{18} in a Ni-Cr sample after two-stage oxidation at 1323 K, illustrating the change in oxidation mechanism



I stage: Ar-20% $^{16}O_2$; 0,5 h
 II stage: Ar-20% $^{18}O_2$; 2 h



I stage: Ar-4% H_2 -2% $H_2^{16}O_2$; 0,5 h
 II stage: Ar-4% H_2 -2% $H_2^{18}O_2$; 2 h

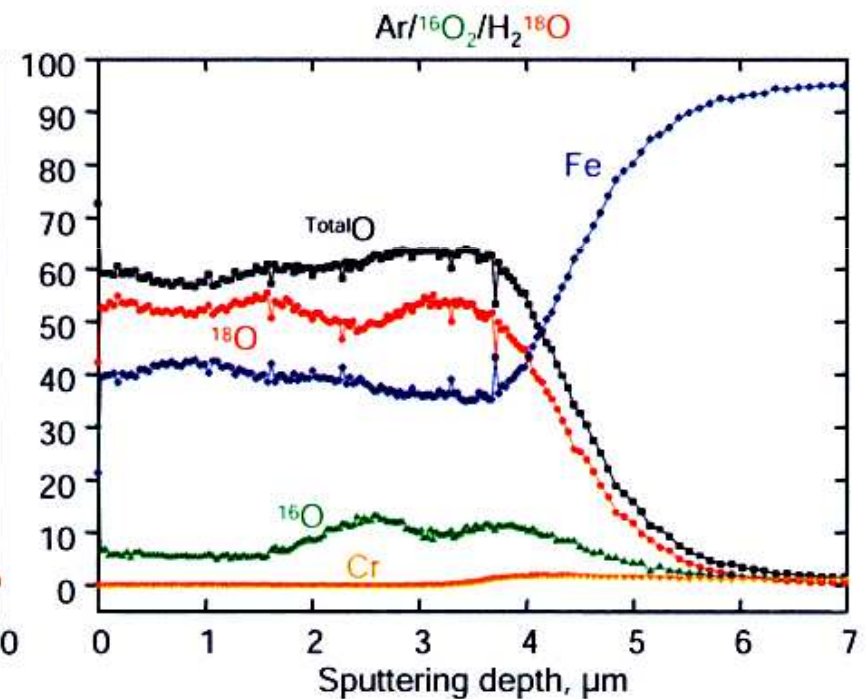
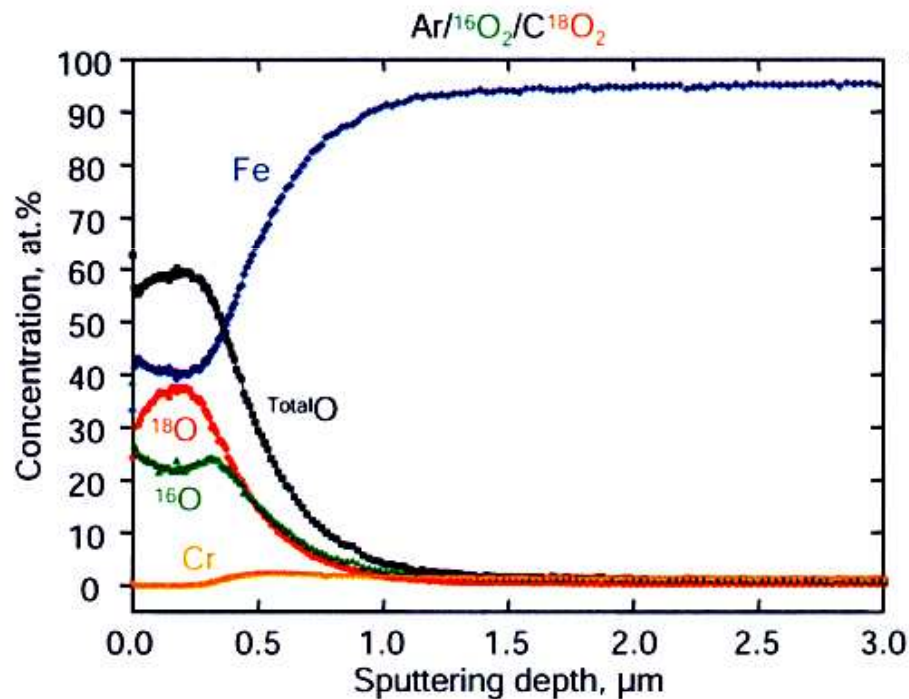
David J. Young, „High temperature oxidation and corrosion of metals”, Elsevier, Sydney 2016

Concentration profiles of Cr, Fe, O¹⁶ and O¹⁸ in a 13CrMo4-4 steel sample after oxidation at 823 K, explaining the influence of water vapor on the oxidation process

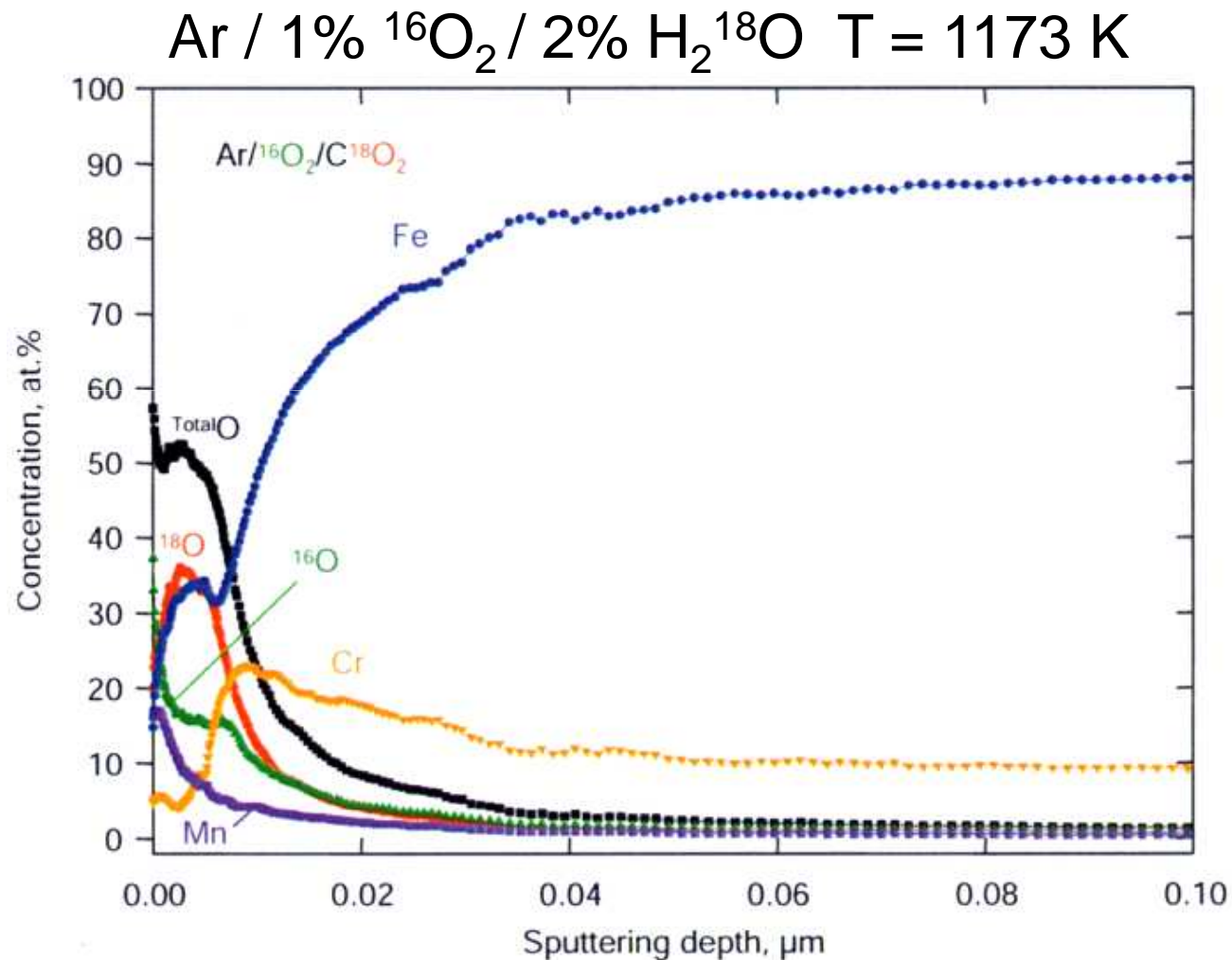


Ar / 1% ¹⁶O₂ / 1% C¹⁸O₂; 2 h

Ar / 1% ¹⁶O₂ / 2% H₂¹⁸O; 2 h



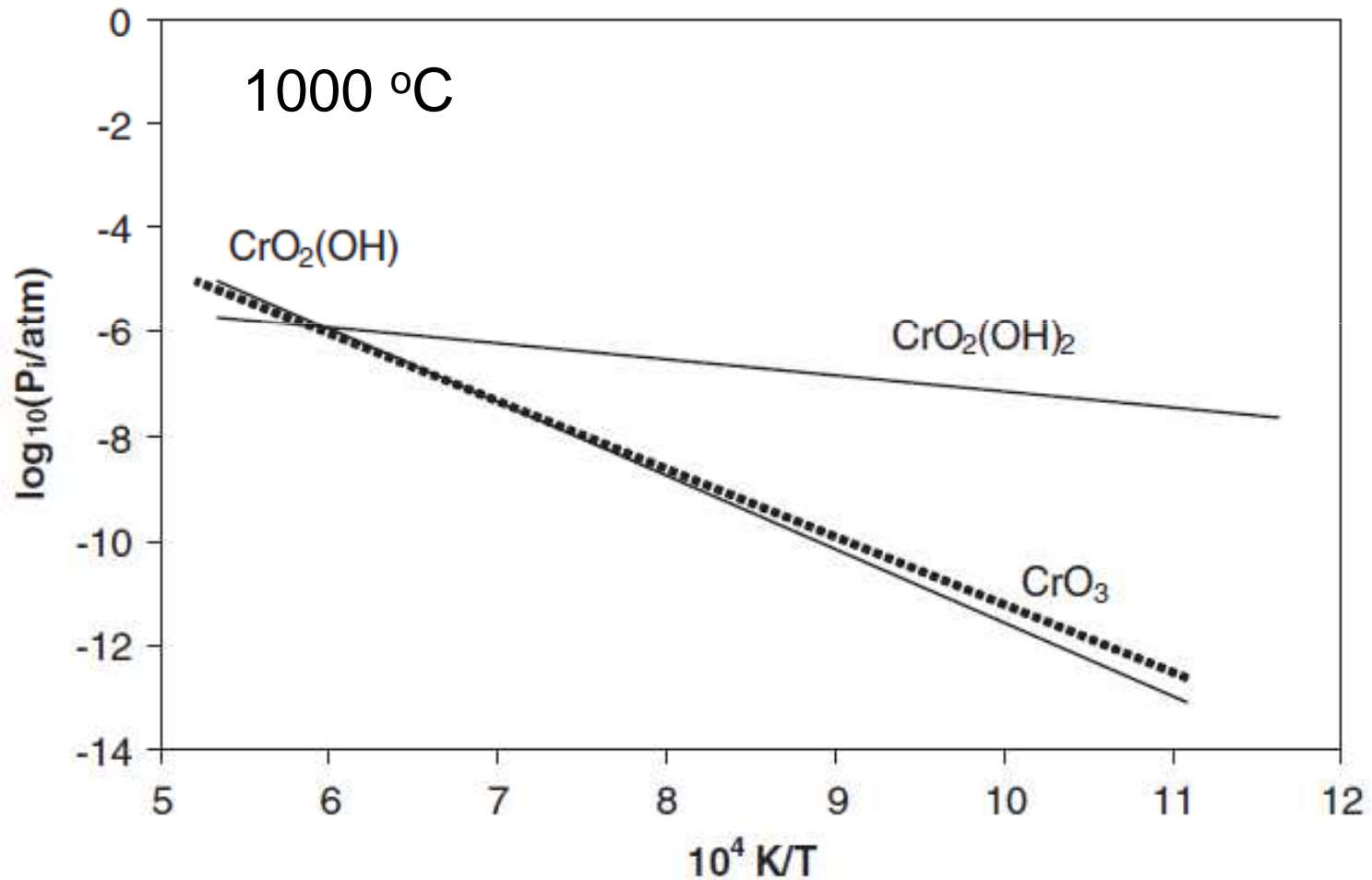
Element concentration profiles in an INCONEL 617 sample after oxidation, explaining the influence of water vapor on the oxidation process



T. Olszewski, „Oxidation mechanisms of materials for heat exchanging components in $\text{CO}_2/\text{H}_2\text{O}$ -containing gases relevant to oxy-fuel environments”, Forschungszentrum Jülich GmbH, Jülich, 2012



Temperature dependence of the pressures of selected volatile chromium oxides and hydroxides at oxygen pressure 0.21 atm and water vapor pressure 0.04 atm



D. J. Young, High temperature oxidation and corrosion of metals, Elsevier, Sydney 2008

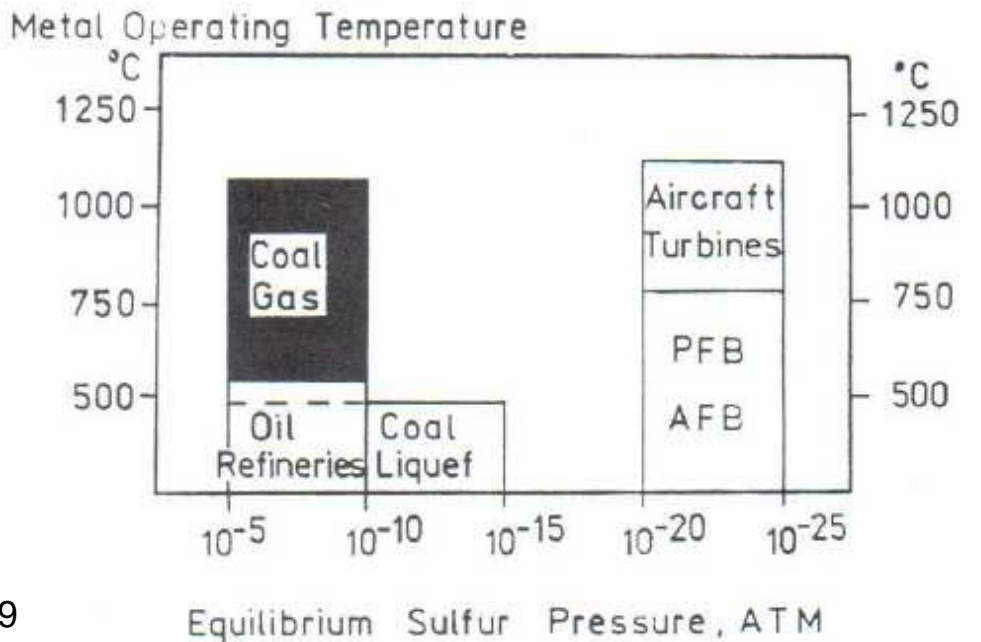
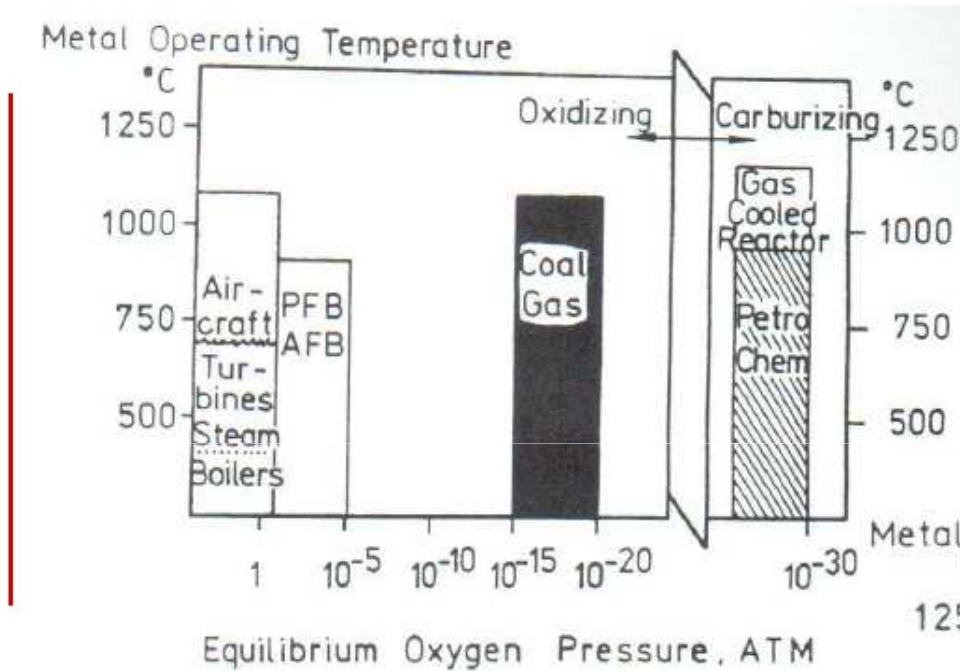
Standard free enthalpy of formation reactions for several metal hydroxides

Table 10.1 Standard free energies of metal hydroxide formation reactions^a

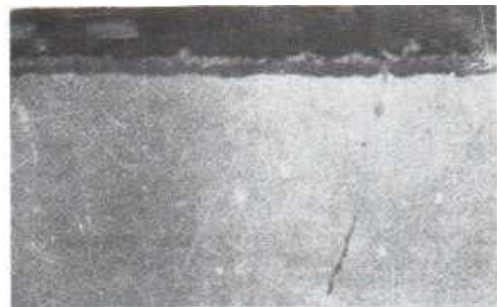
Reaction	$\Delta G^\circ = A + BT$ (J)		Ref.
	A	B	
$\text{FeO(s)} + \text{H}_2\text{O(g)} = \text{Fe(OH)}_2\text{(g)}$	175,700	-31.4	[5]
$\text{Fe}_3\text{O}_4\text{(s)} + 3\text{H}_2\text{O(g)} = 3\text{Fe(OH)}_2\text{(g)} + \frac{1}{2}\text{O}_2\text{(g)}$	818,400	-193	[6]
$\text{Fe}_2\text{O}_3\text{(s)} + 2\text{H}_2\text{O(g)} = 2\text{Fe(OH)}_2\text{(g)} + \frac{1}{2}\text{O}_2\text{(g)}$	663,300	-200	[7]
$\text{NiO(s)} + \text{H}_2\text{O(g)} = \text{Ni(OH)}_2\text{(g)}$	219,000	-50.7	[6]
$\text{Cr}_2\text{O}_3\text{(s)} + 2\text{H}_2\text{O(g)} + \frac{3}{2}\text{O}_2\text{(g)} = 2\text{CrO}_2\text{(OH)}_2\text{(g)}$	53,500	45.5	[8]
$\text{Al}_2\text{O}_3\text{(s)} + 3\text{H}_2\text{O(g)} = 2\text{Al(OH)}_3\text{(g)}$	220,000	-14.7	[9]
$\text{SiO}_2\text{(s)} + 2\text{H}_2\text{O(g)} = \text{Si(OH)}_4\text{(g)}$	47,900	72.3	[10–12]

^aFor mole numbers of reactions as written.

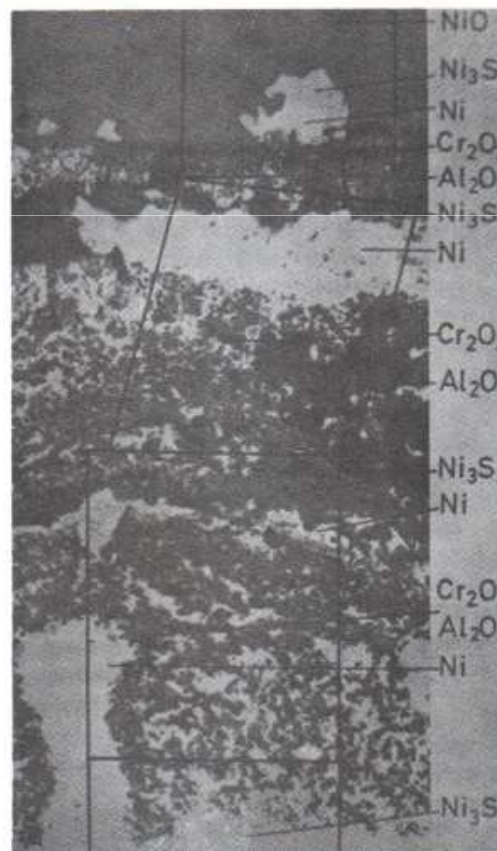
Schematic illustration of sulphidizing-oxidizing atmospheres present in selected branches of modern industry



Cross-sections of scales formed on Ni-9Cr-6Al-0.1Y in two different aggressive atmospheres



Al₂O₃ T = 1000 °C
 Alloy air
 t = 40 h

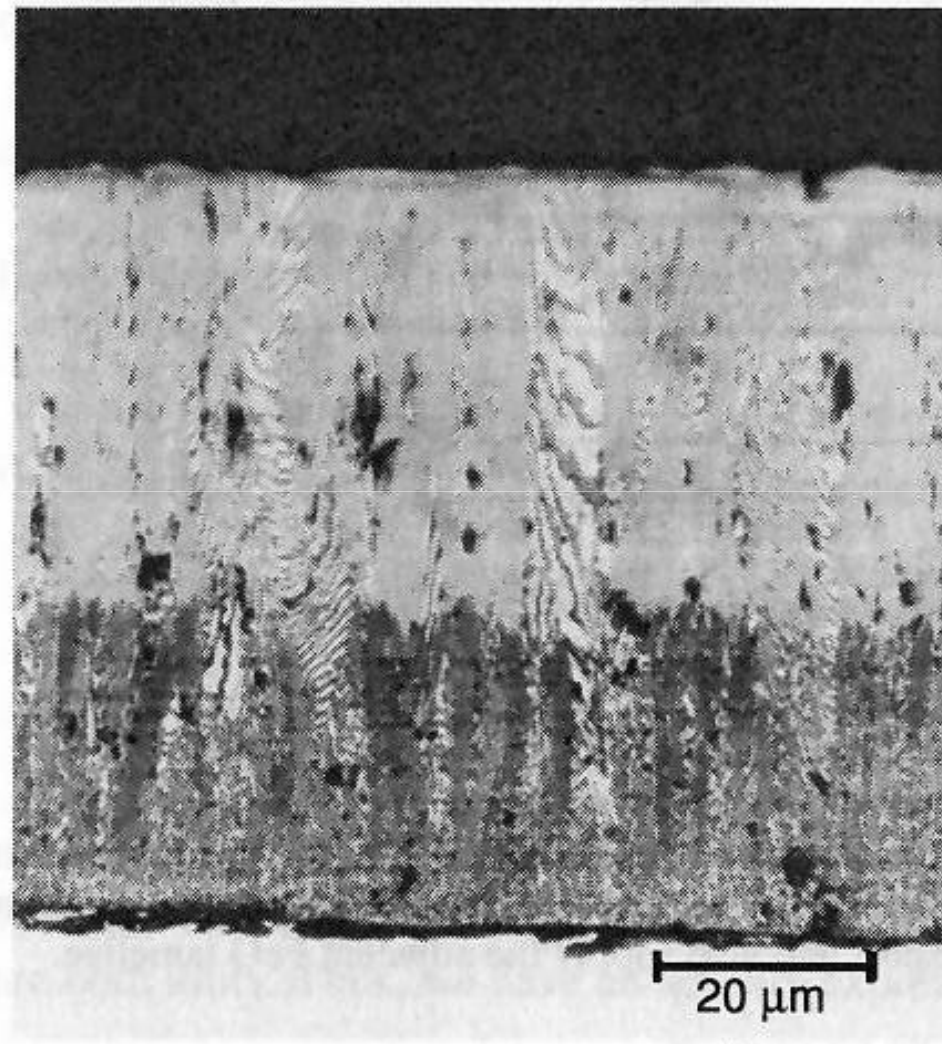


T = 950 °C
 exhaust gases with 550 ppm sulphur
 t = 96 h

Scale

NiO
 Ni₃S₂
 Ni
 Cr₂O₃
 Al₂O₃
 Ni₃S₂
 Ni
 Cr₂O₃
 Al₂O₃
 Ni₃S₂
 Ni
 Cr₂O₃
 Al₂O₃
 Ni
 Ni₃S₂

Cross-section of a sulphide-oxide scale, grown on iron at 900 °C in Ar-1%SO₂ atmosphere



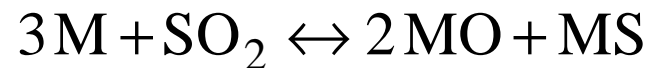
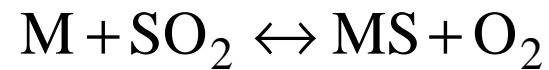
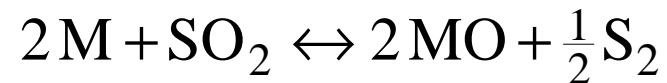
Fe₃O₄ + FeS
duplex

FeO + FeS
duplex

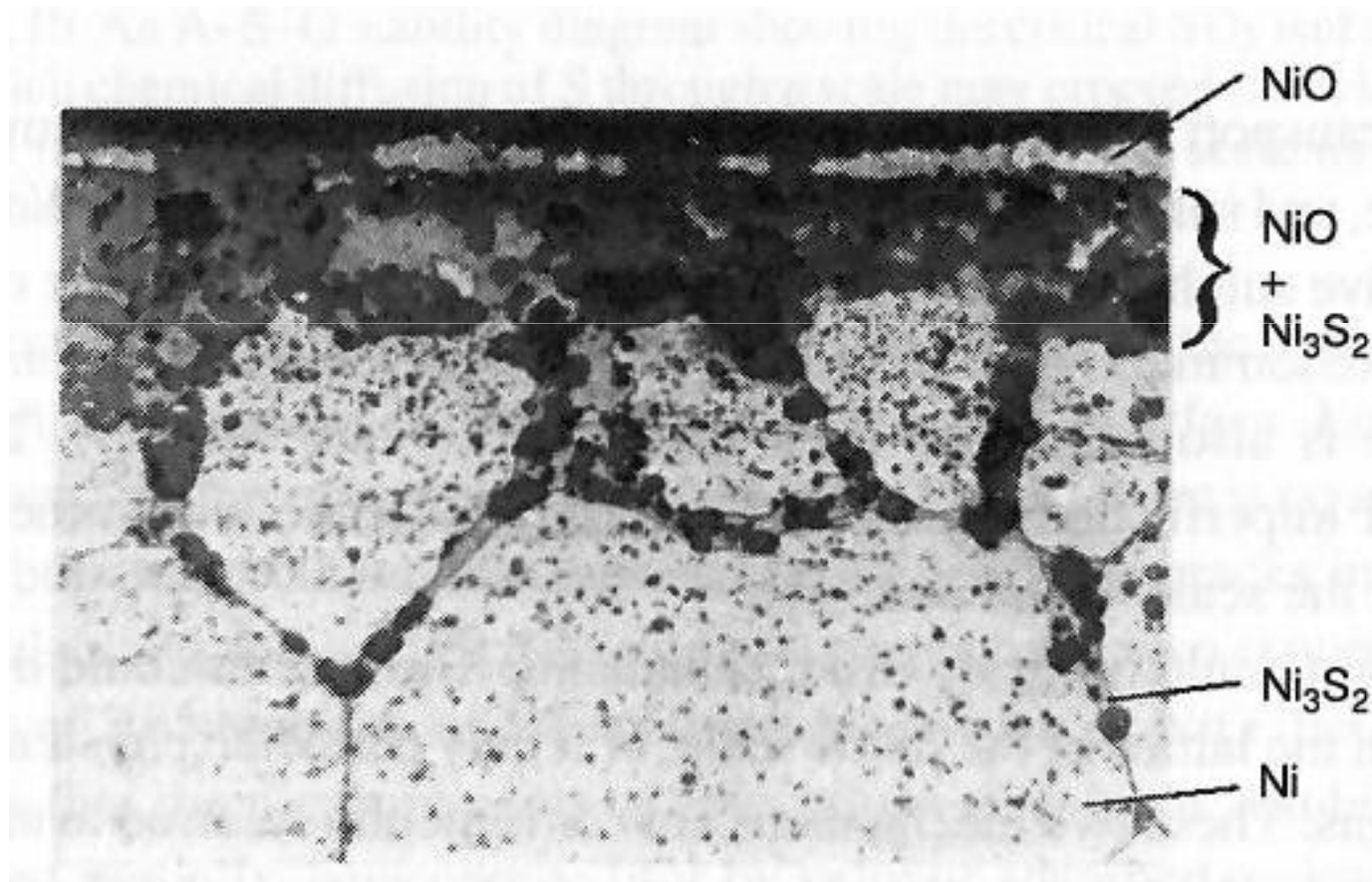
Iron

Formation of metastable sulfides in SO₂ atmosphere

Thermodynamic and kinetic aspects of the formation of complex duplex-type scales in SO₂-containing atmospheres

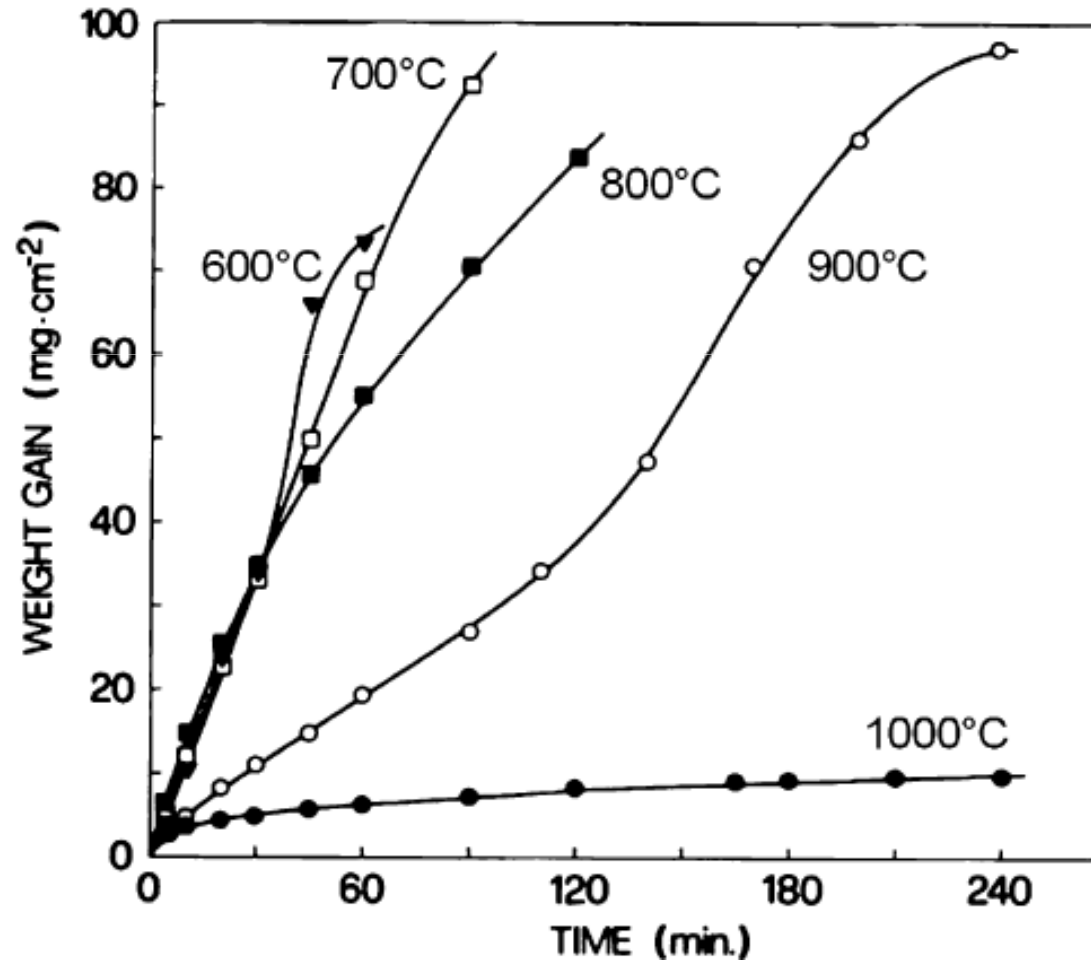


Cross-section of a sulphide-oxide scale, grown on nickel at 1000 °C in SO₂ atmosphere, illustrating substrate penetration along grain boundaries by a liquid eutectic from the Ni-S-O system

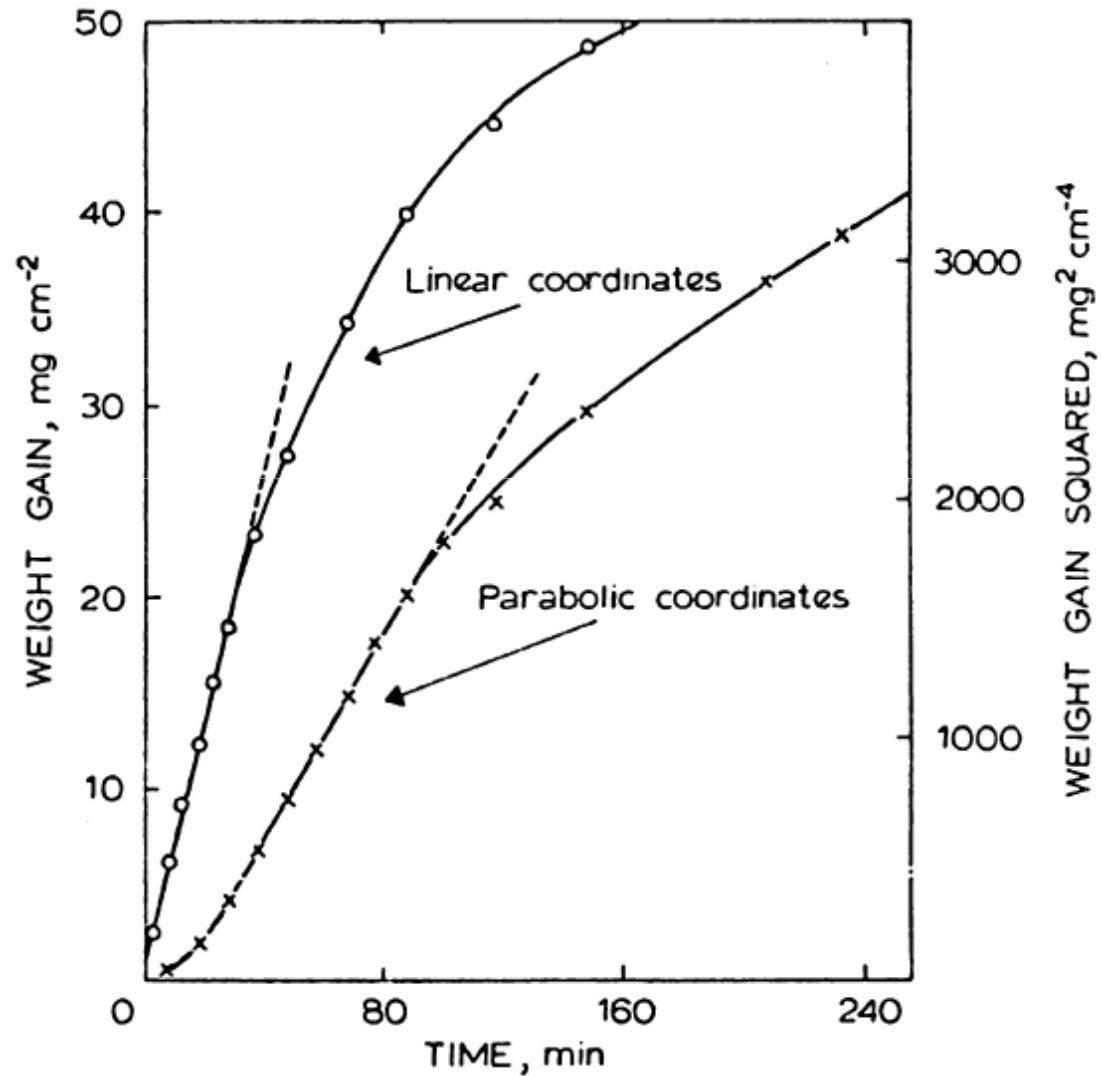


N. Birks, G.H. Meier and F.S Pettit, Introduction to the high temperature oxidation of metals, Cambridge, University Press, 2009.

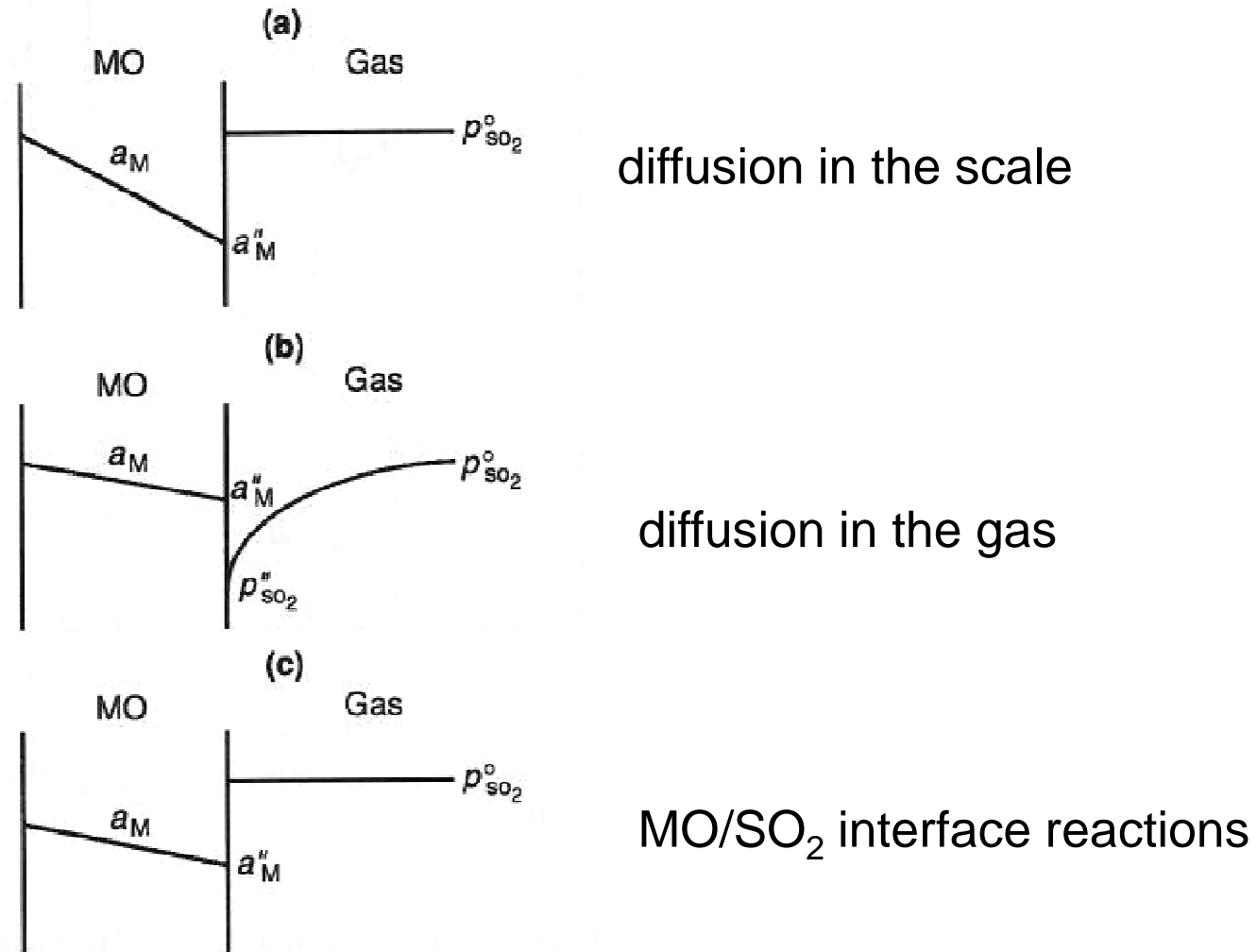
Oxidation kinetics of nickel in SO₂ at selected temperatures



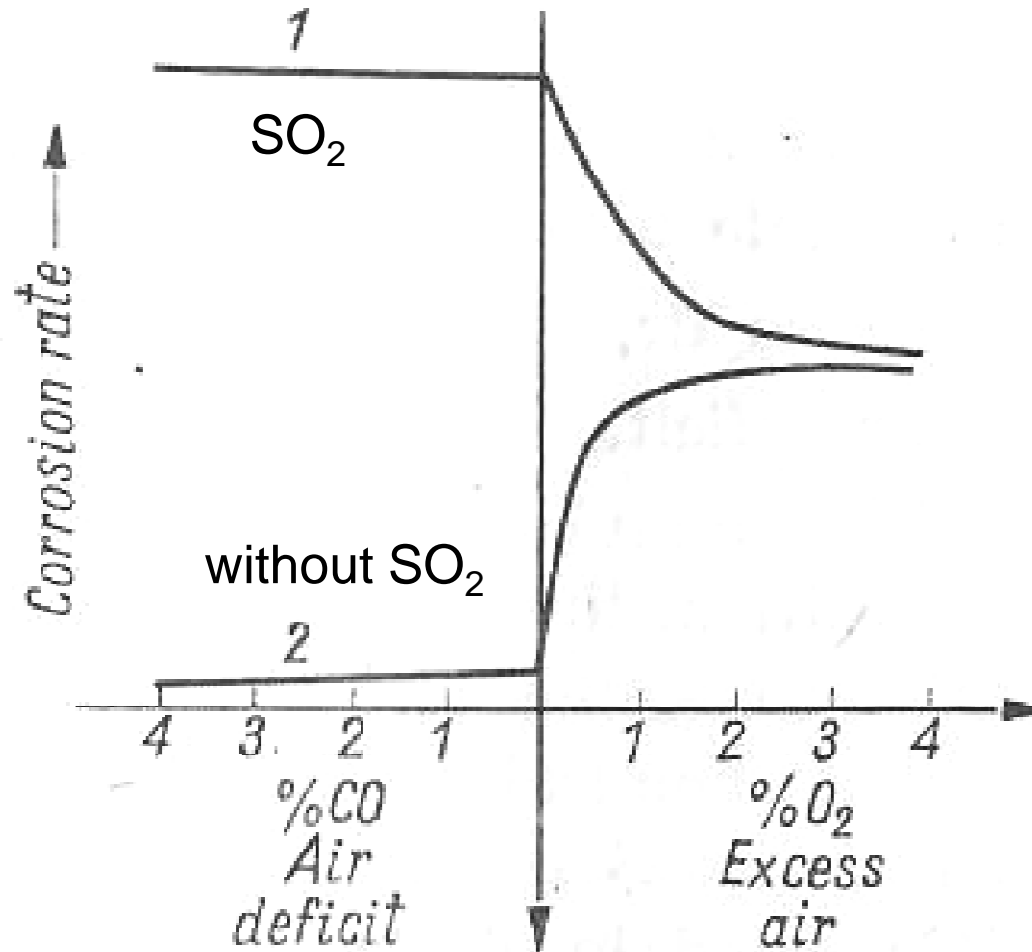
Complex oxidation kinetics of iron in Ar-SO₂ atmosphere (800 °C)



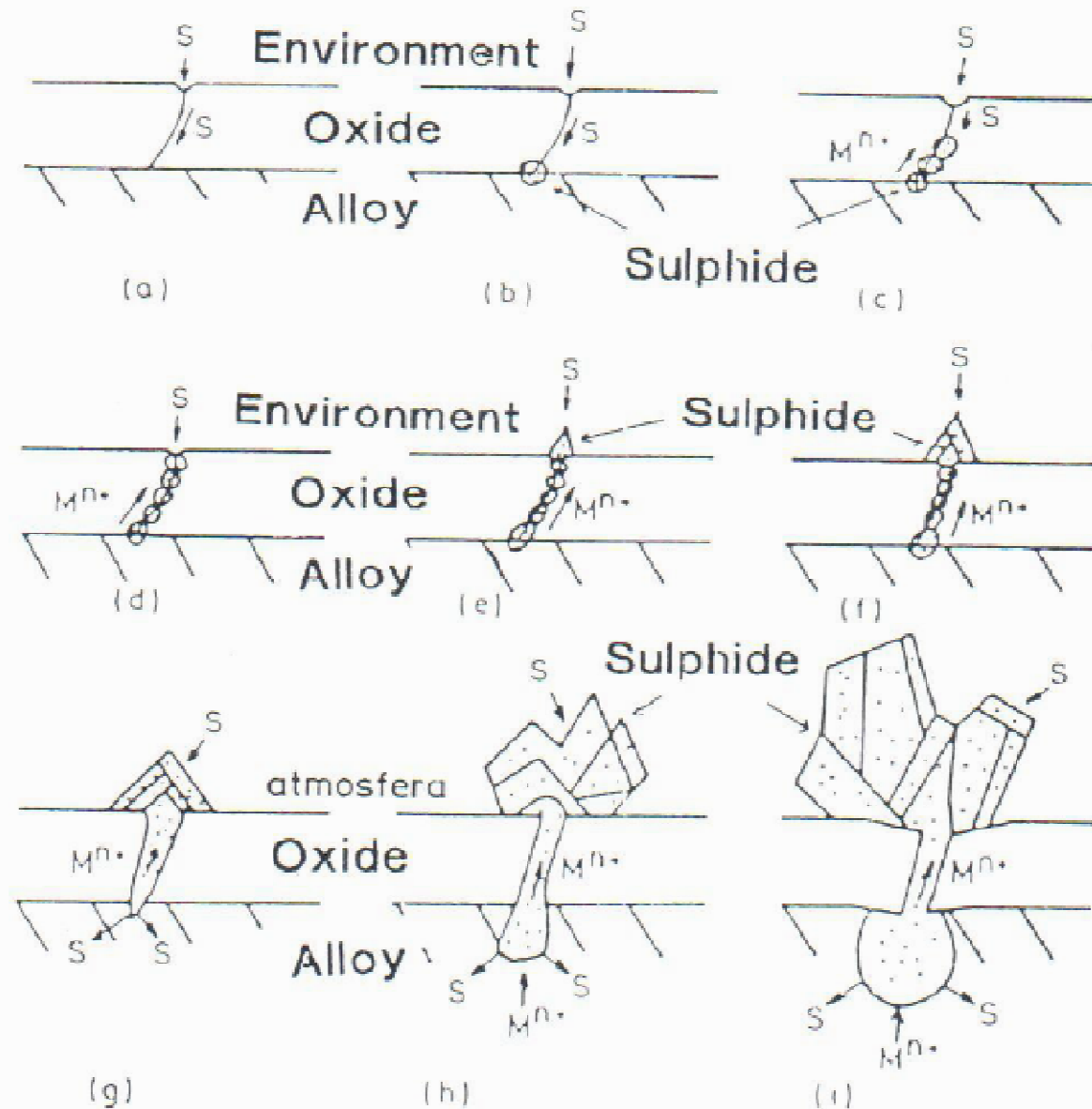
Partial processes that determine the corrosion rate in SO₂ atmosphere



Dependence of the corrosion rate of low-carbon steels in exhaust gases on the presence of SO_2



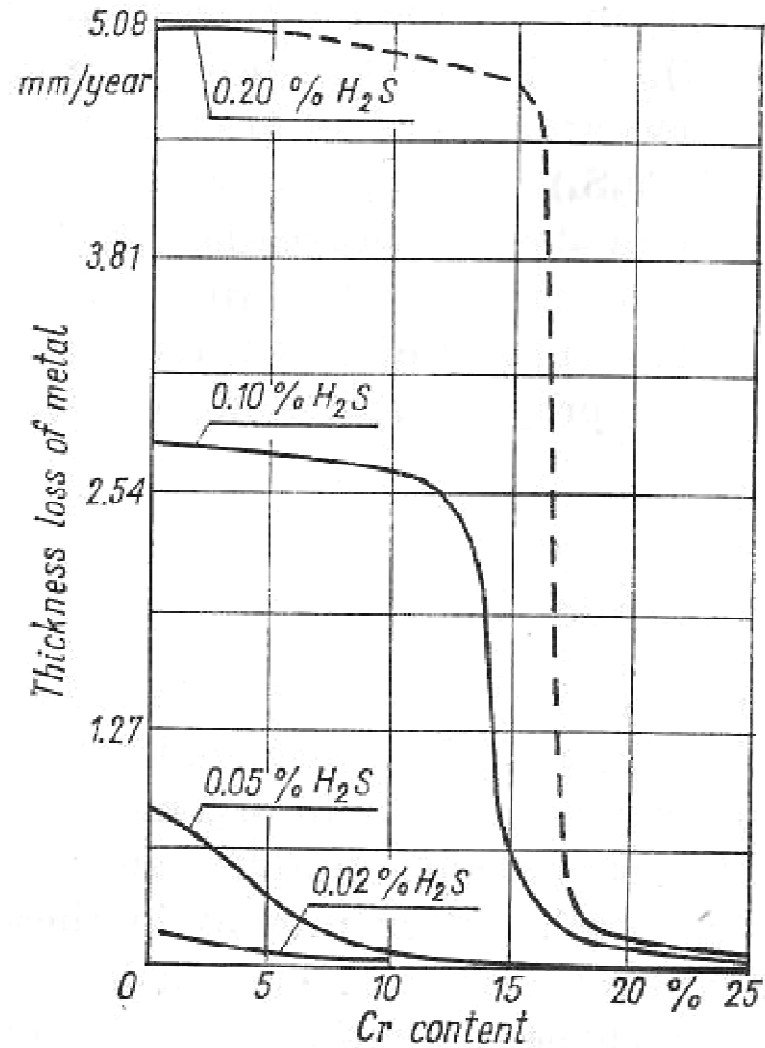
Schematic illustration of the sulphidation of previously oxidized Fe-Cr-Al and Fe-Cr alloys



Influence of H₂S on the corrosion rate of Fe-Cr alloys

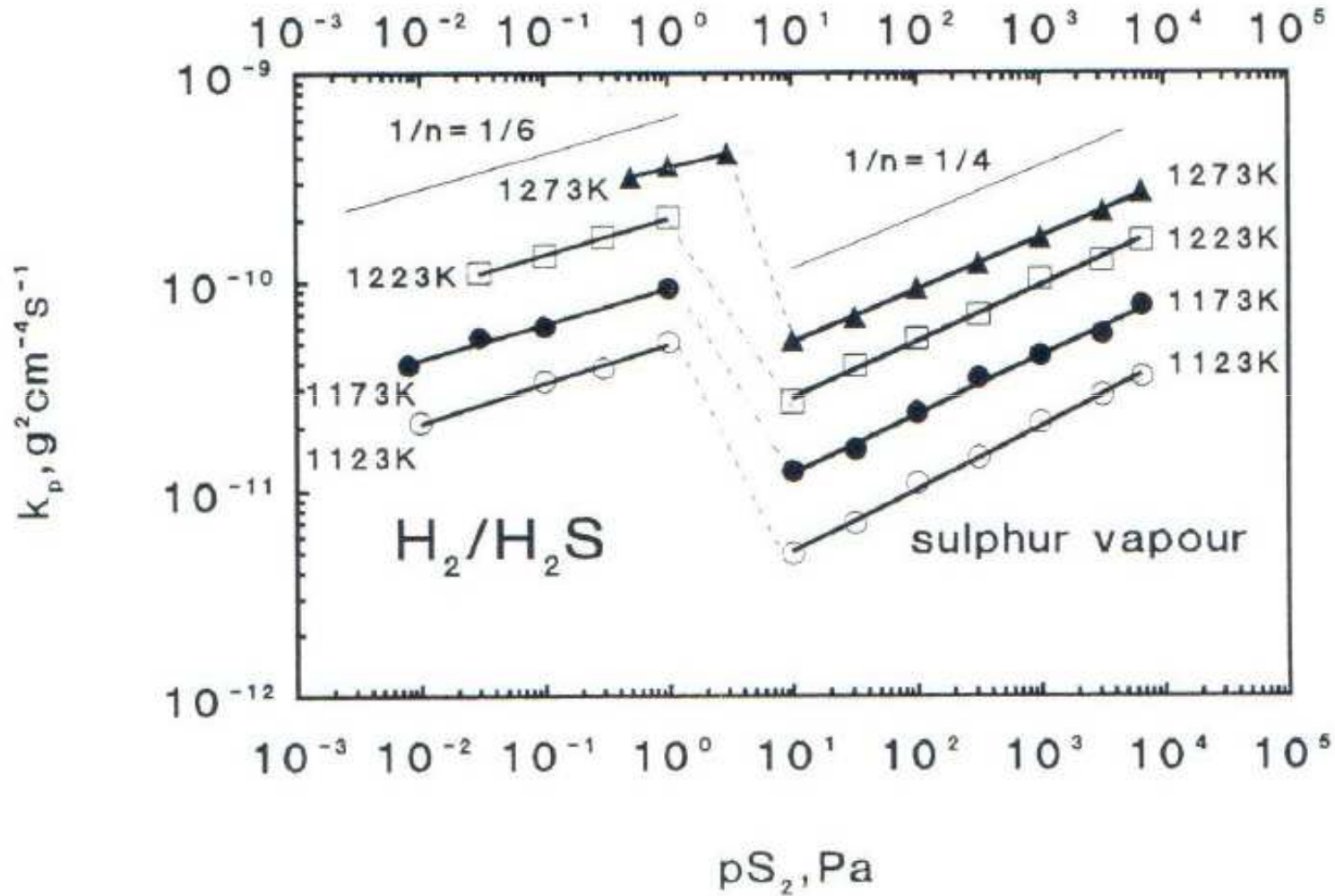


www.agh.edu.pl

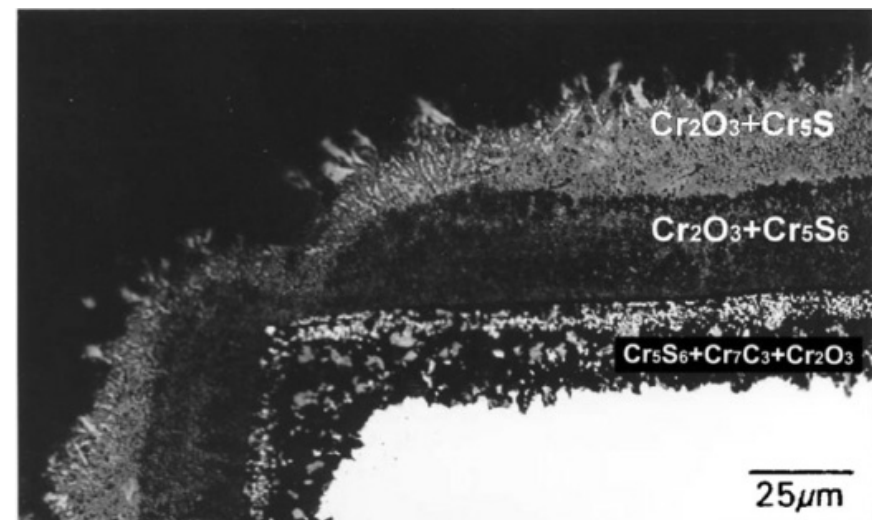
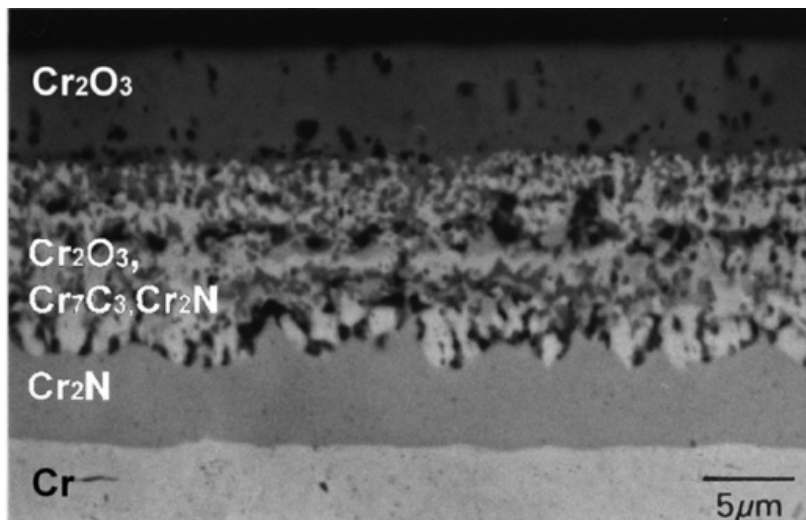
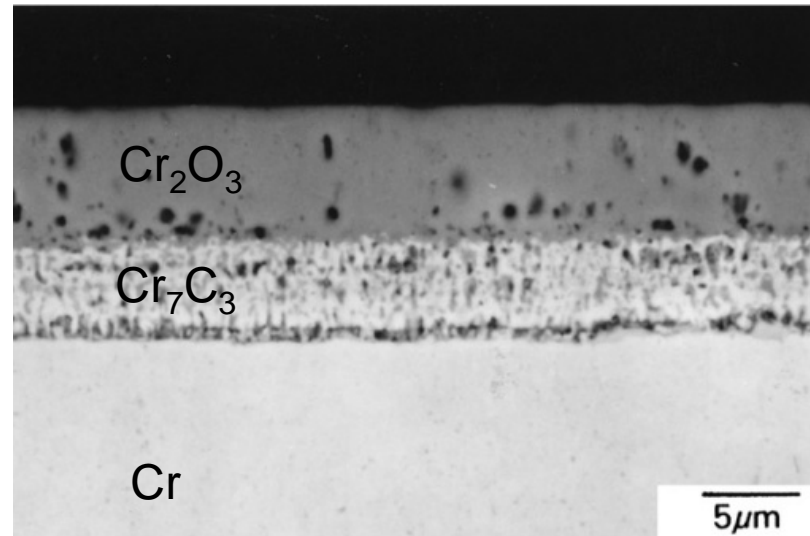


S. Mrowec and T. Werber, Modern Scaling-Resistant Materials, National Bureau of Standards and National Science Foundation, Washington D.C., 1982

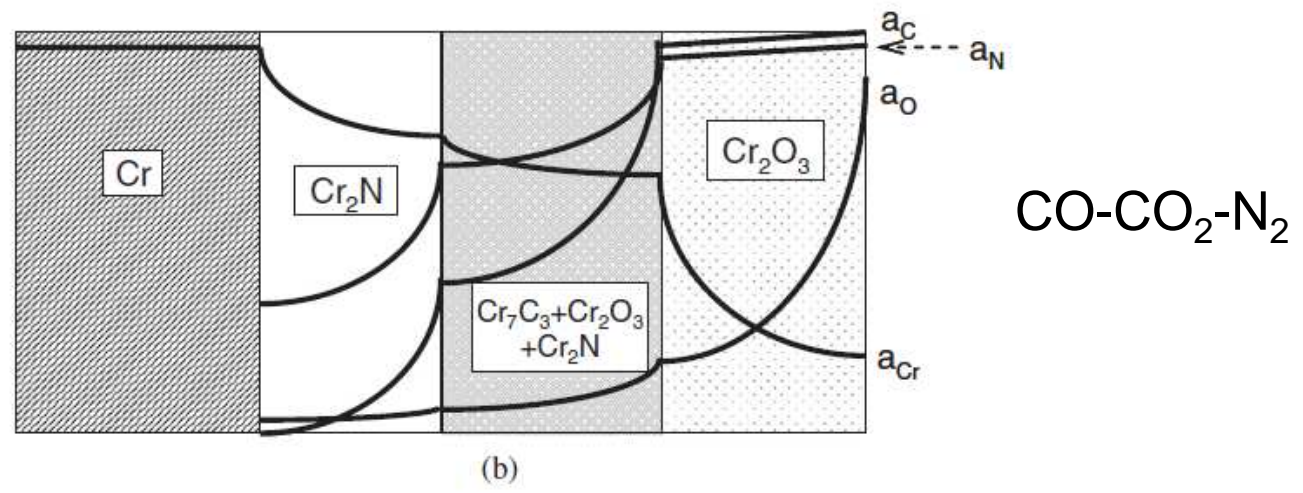
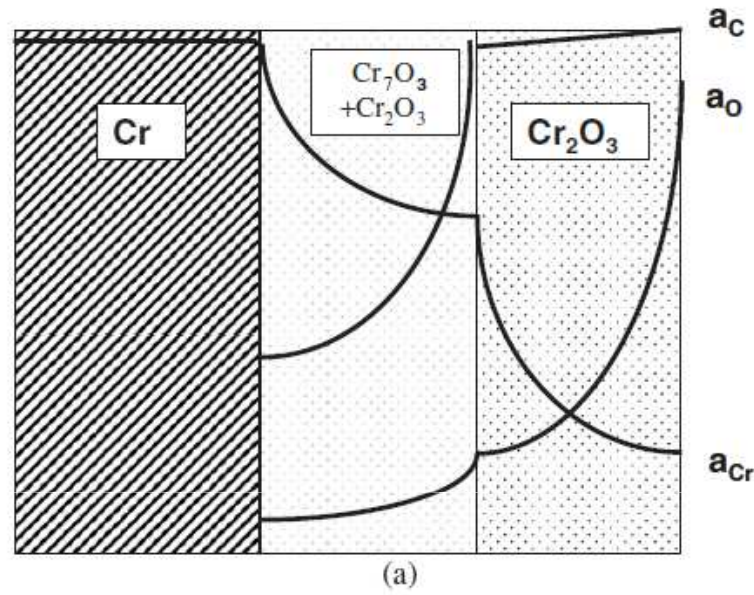
Comparison between the molybdenum sulphidation rate in H_2 - H_2S atmosphere and in sulfur vapors



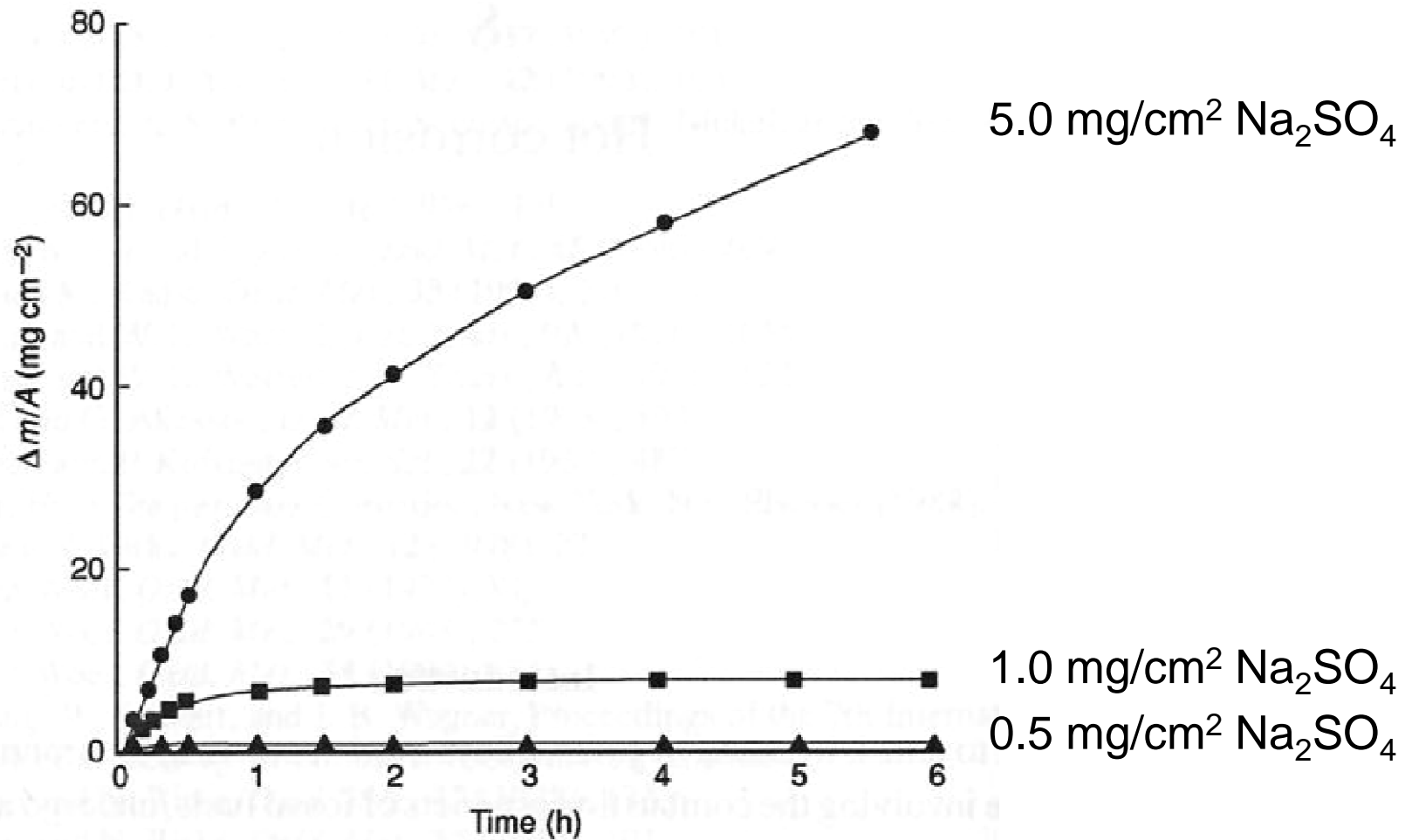
Chromium corrosion in CO-CO₂-containing atmosphere



Schematic illustration of element concentration distribution in a scale formed due to chromium corrosion



Influence of Na_2SO_4 additive on Ni-8Cr-6Al alloy oxidation kinetics at 1000 °C (hot corrosion)



Oxidation kinetics of Ni-8Cr-6Al alloy in the presence of Na₂SO₄ in static and dynamic conditions (1000 °C)

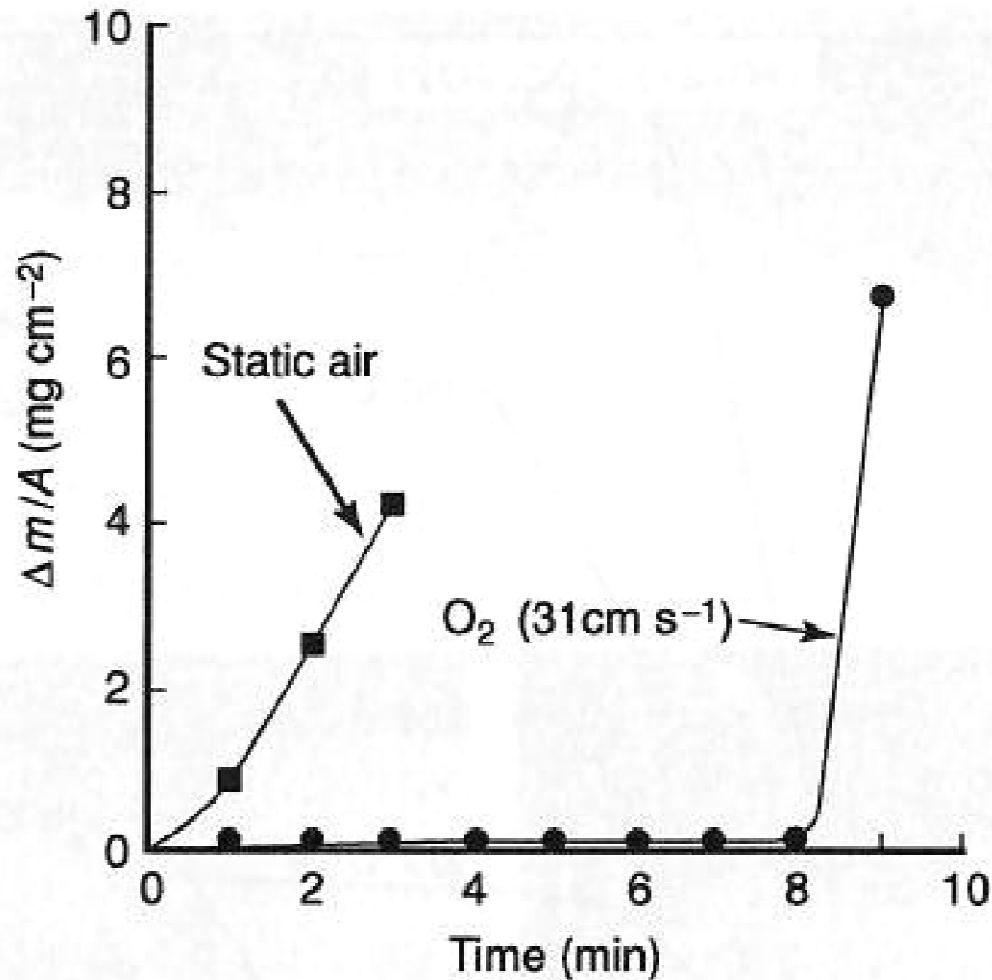
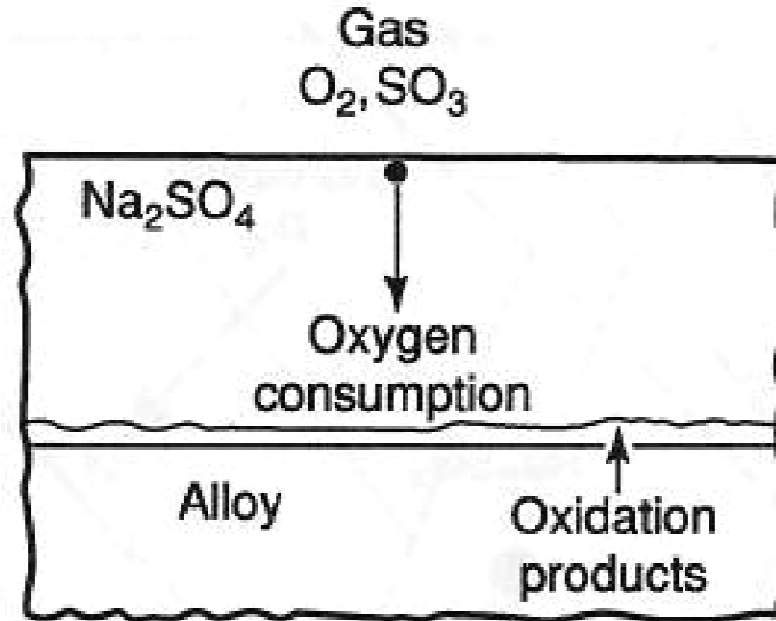
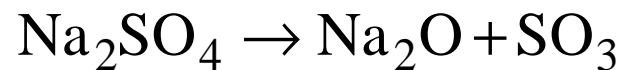


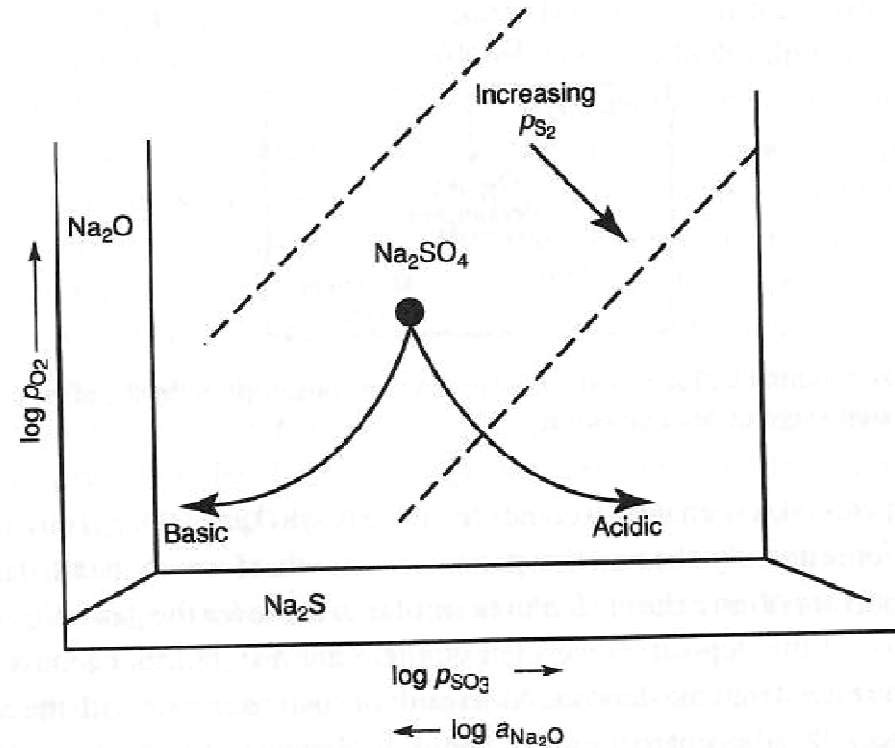
Diagram of the oxygen consumption process during the early stage of corrosion in the presence of Na_2SO_4



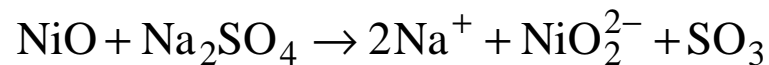
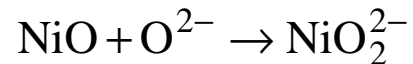
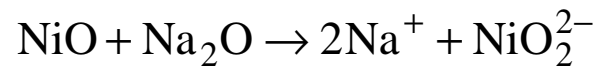
Melting temperature of Na_2SO_4 : 884 °C



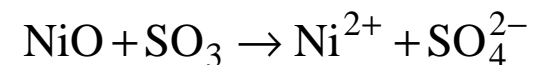
Schematic diagram of Na-O-S system stability



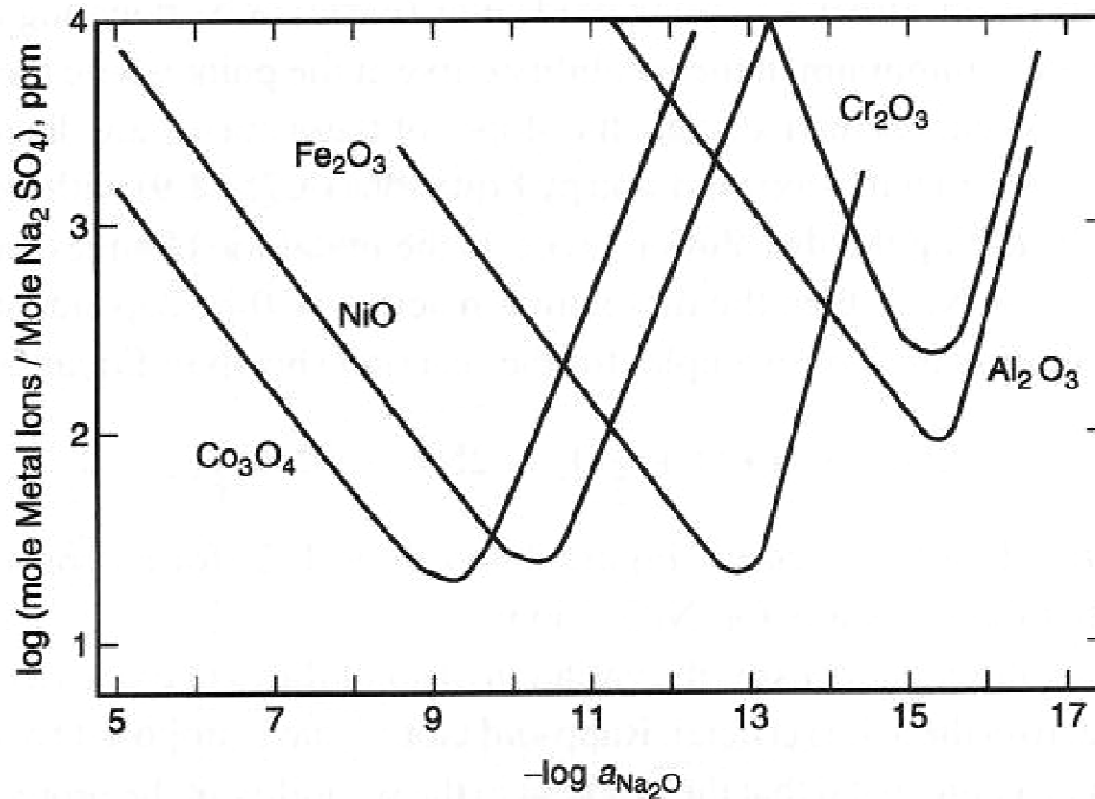
alkaline mode:



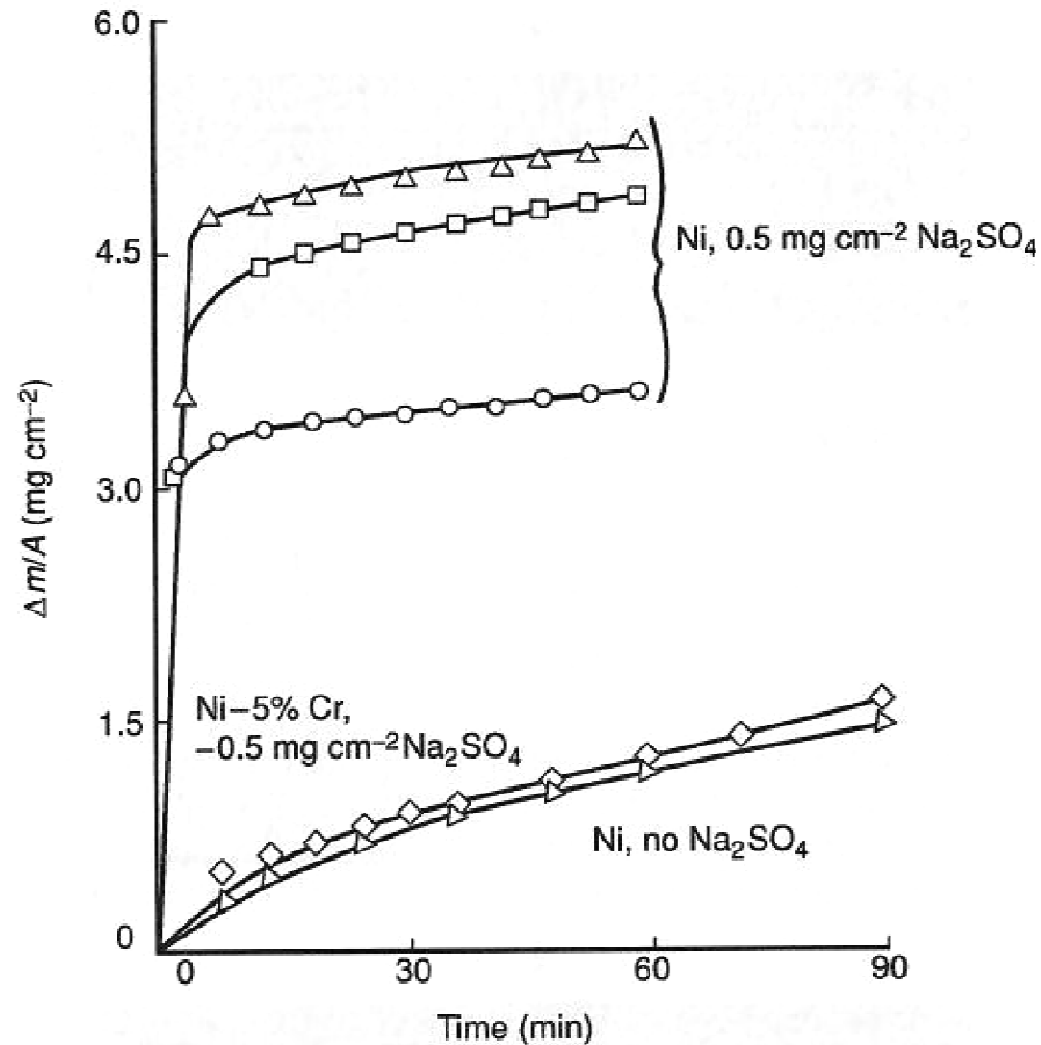
acidic mode:



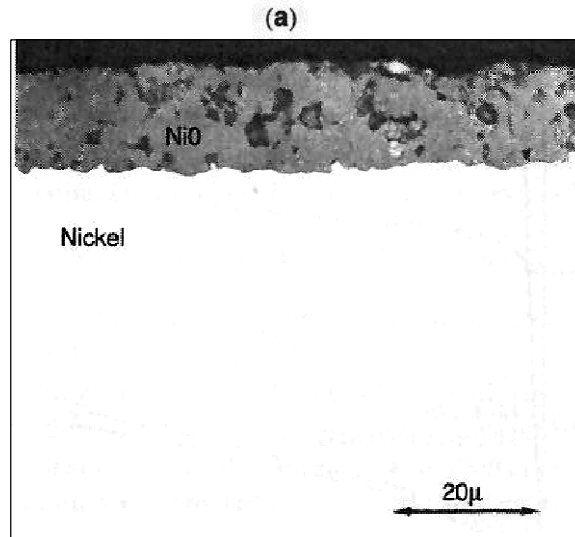
Solubility of selected oxides in Na_2SO_4 at 1200 K, at oxygen pressure equal to 1 atm



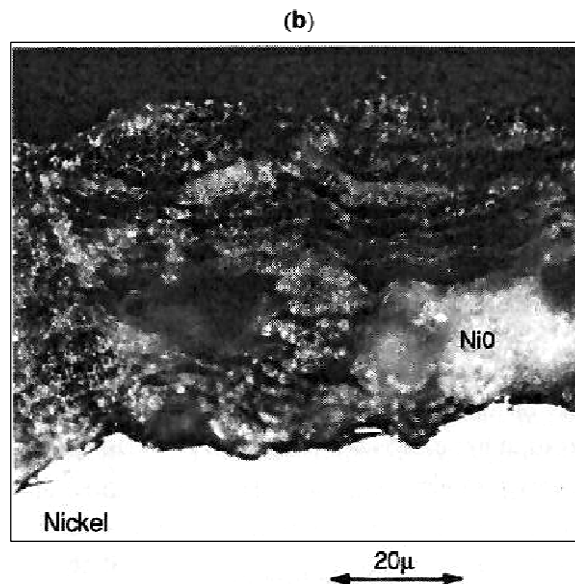
Influence of Na_2SO_4 additive on oxidation kinetics of nickel and Ni-5%Cr alloy



Cross-section of a scale grown on nickel oxidized in different conditions (1000 °C)



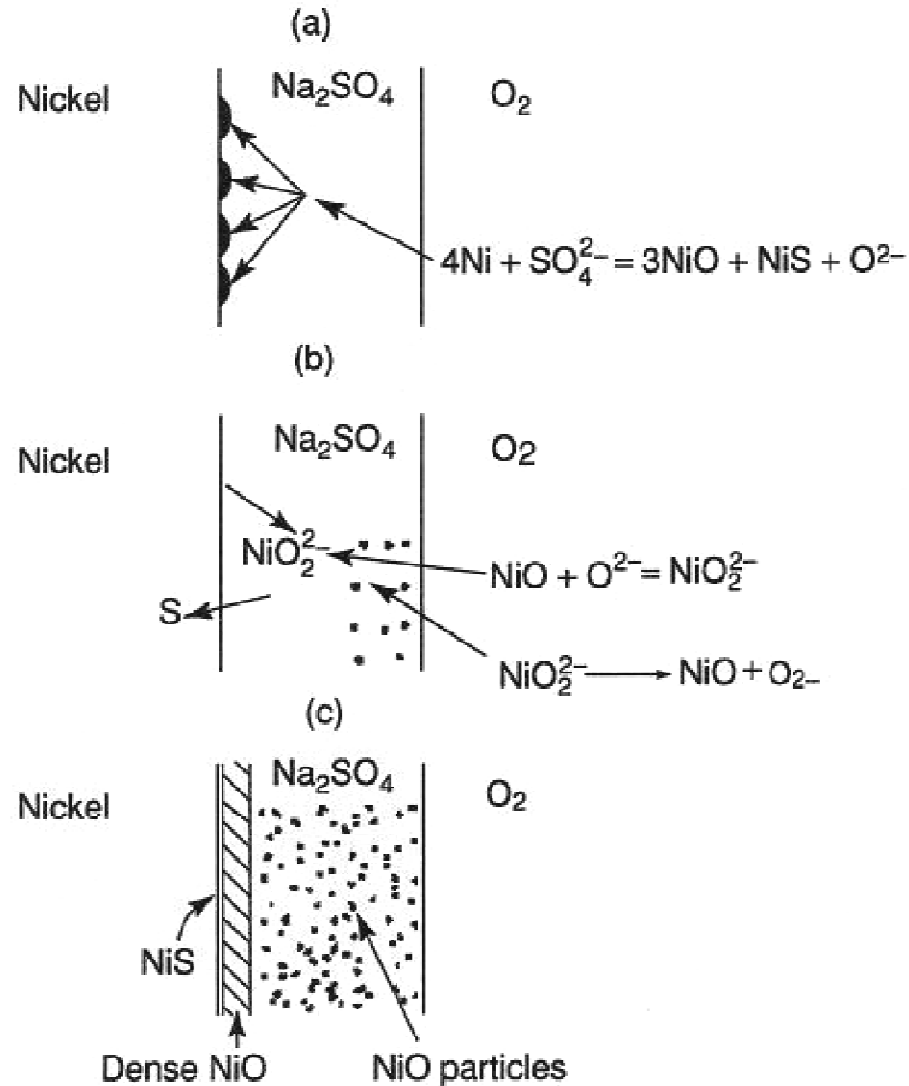
air
t = 3 h



air + 0.5 mg/cm² Na₂SO₄
t = 1 min

N. Birks, G.H. Meier and F.S Pettit, Introduction to the high temperature oxidation of metals, Cambridge, University Press, 2009.

Model of nickel corrosion in the presence of Na_2SO_4



Salts present in gas turbines

Salt Constituent	Deposit Chemistry (mole %)	
	First Stage	Second Stage
External Airfoil Surface		
Na ₂ SO ₄	40	28
K ₂ SO ₄	4	3
CaSO ₄	40	59
MgSO ₄	13	8
Internal Cooling Passages		
Na ₂ SO ₄	45	37
K ₂ SO ₄	3.2	4.4
CaSO ₄	41	46
MgSO ₄	9.5	11.5

Salts present in sea water

Salt Constituents	Concentration, g/L (%)
NaCl	23 (52)
MgCl ₂ 6H ₂ O	11 (25)
KCl, KBr	1.1 (2)
CaCl ₂ 2H ₂ O	1.4 (3)
Na ₂ SO ₄ 10H ₂ O	8 (18)
Total	44.5 (100)



THE END